Beach and Dune Analysis Using Chiroptera Imaging System, South Padre and Brazos Islands, Texas Gulf Coast

Tiffany L. Caudle, Thomas A. Tremblay, Jeffrey G. Paine, John R. Andrews and Kutalmis Saylam

Final Report

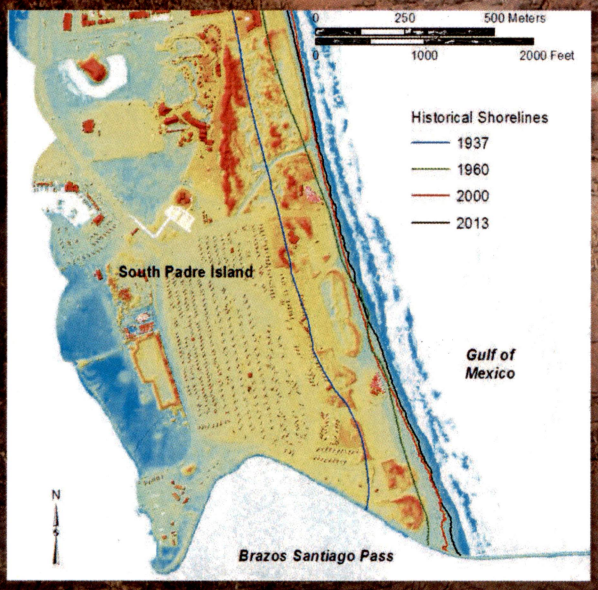

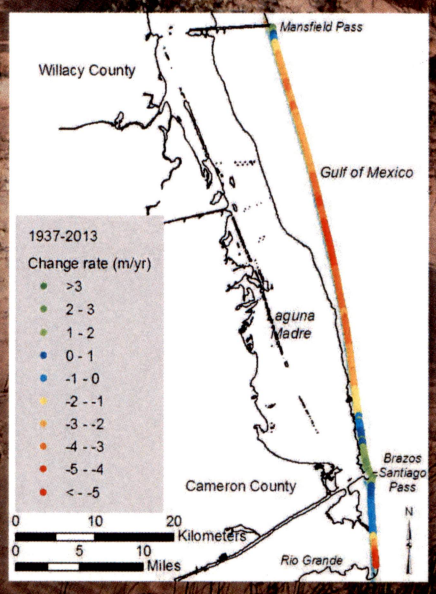

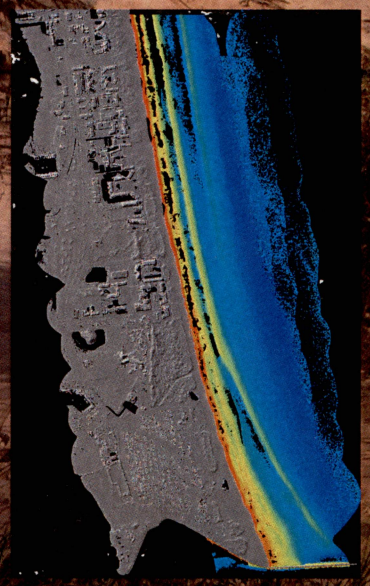

Bureau of Economic Geology
Scott W. Tinker, Director
John A. and Katherine G. Jackson School of Geosciences
The University of Texas at Austin
Austin, Texas 78713-8924

A Report of the Coastal Coordination Council Pursuant to National Oceanic and Atmospheric Administration Award No. NA12NOS4190021

Final Report Prepared for General Land Office under contract no. 13-030-000-6895.

QAe2830

Final Report

Beach and Dune Analysis Using Chiroptera Imaging System, South Padre and Brazos Islands, Texas Gulf Coast

Tiffany L. Caudle, Thomas A. Tremblay, Jeffrey G. Paine,
John R. Andrews and Kutalmis Saylam

Report to the Texas Coastal Coordination Council pursuant to
National Oceanic and Atmospheric Administration Award No. NA12NOS4190021.

Final report prepared for General Land Office under contract No. 13-030-000-6895.

Bureau of Economic Geology
Scott W. Tinker, Director
Jackson School of Geosciences
The University of Texas at Austin
Austin, Texas 78713-8924

June 2014

QAe2830

CONTENTS

Abstract 1
Introduction 2
Methods 6
Data Acquisition 6
Lidar Data Processing 8
Topographic Processing 10
Bathymetric Processing 10
Aerial Imagery Post-Processing 11
GIS Data Deliverables 13
Shoreline 13
Potential Vegetation Line 16
Landward Dune Line 16
Long-Term Shoreline Change Rates 19
Geomorphic Units 22
Maximum Dune Crest Position and Volume Statistics 25
Barrier Island Geomorphology 27
Shoreline Change 32
Long-Term Change, 1937–2013 33
Decadal Change, 2000–2013 35
Short-Term Change, 2010–2013 38
Comparison of Historical, Decadal, and Short-Term Periods 41
Volumetric Analysis 44
Bathymetric Lidar Assessment 52
Conclusions 56
Acknowledgments 57
References 59
Appendix A: Imagemagick Script 61
Appendix B: Threshold Elevation Curves-Survey Comparison 62
Appendix C: Threshold Elevation Curves-Shoreline Segment Change 64
Appendix D: Data Volume Contents 67

FIGURES

1. Index map of the study area 5

2. Trajectories of all three flights showing coverage between Mansfield Channel and Rio Grande 9

3. Merged topographic and bathymetric digital elevation model (DEM) for area north Brazos Santiago Pass 12

4. 2013 shoreline and potential vegetation line positions on South Padre Island 15

5. Location of landward dune boundary in north and south sections of study area 18

6. Sample of historical shoreline positions at Isla Blanca Park on South Padre Island 20

7. Long-term change rates in north and south sections of study area 21

8. Geomorphic units within north and south sections of the study area. 23

9. First appearance of incipient dunes north of Brazos Santiago Pass 24

10. Maximum dune crest elevations along north and south sections of study area 26

11. Generalized barrier island profile illustrating prominent features. 27

12. Storm washover channel 28

13. Active dune and deflation area 28

14. Marsh in depression lagoonward of fore-island dune ridge 29

15. Wind-tidal flats 30

16. Marsh vegetation along margins of a storm washover channel on South Padre Island 30

17. Generalized cross section of Padre Island barrier system 32

18. Geomorphic unit area in South Padre Island study area 32

19. Net rates of long-term change for South Padre Island and Brazos Island calculated from shoreline positions from 1937 through 2013 34

20. Net rates of decade-scale change for South Padre Island and Brazos Island calculated from shoreline positions from 2000 through 2013 37

21. Net shoreline change between April 2010 and February 2013 for South Padre Island and Brazos Island 39

22. Short-term shoreline change between Rio Grande and Mansfield Channel showing fluctuations between advance and retreat 41

23. Comparison of historical and decade-scale net shoreline change rates (m/yr) with short-term net shoreline movement (m) 43

24. Changes in shoreline position, vegetation line position, and sediment volume at SPI02 on South Padre Island as measured by Port Isabel High School students participating in Texas High School Coastal Monitoring Program 43

25. Average volume ($m^{3/}m$) of sand per meter of shoreline above threshold elevations in 2000, 2010, and 2013 for Brazos and South Padre Islands 45

26. Average volume (m^3/m) above threshold elevations for Brazos and South Padre Island and South Padre Island segments calculated from 2013 lidar-derived DEMS 47

27. South Padre Island developed segment with seawall displaying maximum dune crest elevations 48

28. Developed segment of South Padre Island with seawall showing maximum dune crest elevations 49

29. Undeveloped South Padre Island showing maximum dune crest elevations 50

30. Average volume (m^3/m) of sand per meter of shoreline above threshold elevations in 2000, 2010, and 2013 for developed area of South Padre Island without seawall 51

31. Single-beam sonar lines collected October 2012 53

32. Comparison of lidar (blue) with single-beam sonar (red) from southernmost transect line near north jetty of Brazos Santiago Pass 54

33. Comparison of lidar bottom returns (blue) with sonar data points (red) from northernmost transect 55

34. Comparison of waveform returns in clear water with two strong peaks representing water surface and seafloor with noisy waveform pattern in murky water 55

TABLES

1. Comparison of historical (1937–2013) and decadal (2000–2013) shoreline change rates for South Padre and Brazos Islands 36

2. Net shoreline change determined from shoreline position extracted from airborne lidar data acquired in April 2010 and February 2013 40

3. Total combined volume of sand above threshold elevations in beach and dune system on Brazos and South Padre Islands 45

Beach and Dune Analysis Using Chiroptera Imaging System, South Padre and Brazos Islands, Texas Gulf Coast

ABSTRACT

In early 2013 the Bureau of Economic Geology (BEG) acquired lidar data and color infrared (CIR) aerial imagery of South Padre Island and Brazos Island, Texas (Mansfield Channel to Rio Grande), to (1) evaluate position of the shoreline, vegetation line, and back dune line; (2) map geomorphic units; (3) extract maximum dune crest elevations; (4) calculate rates of long-term shoreline change; and (5) provide beach–dune system volume analysis. Data were collected using the BEG's Chiroptera airborne system, which collects topographic lidar data, shallow bathymetric lidar data, and natural color/color infrared imagery. Topographic data and CIR images were collected for a 500-m swath (three passes) of South Padre Island landward of the shoreline. Bathymetric data were collected from the shoreline 1000 m seaward. The bathymetric data-collection portion of this project was intended to establish the depth-penetration and water-clarity limitations of Chiroptera on the open Gulf of Mexico coast. The lidar data and CIR imagery can be used for numerous scientific and coastal-monitoring purposes, including mapping of geomorphic units, quantifying shoreline change, and analyzing beach and dune system volumes.

Geomorphic units along South Padre Island, which are mapped by combining CIR aerial imagery and topographic lidar data, consist of wetland and upland habitats. Wetland habitats are interpreted from BEG-captured 2013 CIR aerial imagery and follow the National Wetlands Inventory (NWI) classification. Upland geomorphic units are mapped from CIR imagery draped on lidar digital elevation models to aid geomorphologic mapping. Upland units include washover channel and fan, fore-island dune complex, fore-island dune ridge, vegetated barrier flat, mid-island dune complex, and back-island dune complex.

A 2013 shoreline position was extracted from the topographic lidar dataset and compared with shoreline positions from 1937 through 2013 for historical, decade-scale, and short-term

shoreline-change analysis. Historical rates of long-term Gulf shoreline change for South Padre Island and Brazos Island averaged 2.2 m/yr of retreat, with 86 percent of sites retreating. Rates decreased over the last decade (2000 to 2013) to 1.1 m/yr of retreat (76 percent of sites retreating). The trend changed between 2010 and 2013, with 64 percent of monitoring sites advancing at an average distance of 4.9 m.

Beach and dune volumes above threshold elevations ranging from 1 to 6 m were extracted from the DEMs to assess geographic and temporal patterns of sand storage. The undeveloped area of South Padre Island had 2 to 4 times the volume of sand at lower threshold elevations than did the heavily developed southernmost section of the island. The volume was 7 times greater at the higher elevation thresholds (5 and 6 m). A constant trend across all the shoreline segments is that volume is reduced by approximately half with each 1-m increase in threshold elevation. In comparisons with earlier lidar datasets, beach and dune system volume in the study area has steadily increased since 2000.

Analysis of the nearshore bathymetric lidar data revealed definitive seafloor returns adjacent to the north jetty at Mansfield Channel and the north jetty at Brazos Santiago Pass. Both of these locations exhibited less suspended sediment in the water column at the time of the survey than the rest of the study area. Further analysis of the bathymetric waveforms in the remainder of the survey area will focus on reducing false classification of water-column returns as seafloor returns through joint development of "murky water" algorithms with the instrument manufacturer.

INTRODUCTION

The Texas coastal zone (fig. 1) is among the most dynamic environments on Earth. Shoreline position is a critical parameter that reflects the balance among several important processes, including sea-level rise, land subsidence, sediment influx, littoral drift, and storm frequency and intensity. Because the Texas coast, and especially South Padre Island, faces ever-increasing developmental pressures as the coastal population swells, an accurate and frequent analysis of

shoreline change serves as a planning tool to identify areas of habitat loss; better quantify threats to residential, industrial, and recreational facilities and transportation infrastructure; and help understand the natural and anthropogenic causes of shoreline change.

The latest trends in shoreline change rates are a critical component in understanding the potential impact that sea level, subsidence, sediment supply, and coastal engineering projects might have on sensitive coastal environments such as beaches, dunes, and wetlands. Rapidly eroding shorelines threaten coastal habitat and recreational, residential, transportation, and industrial infrastructure and can also significantly increase the vulnerability of coastal communities to tropical storms. Repeated, periodic assessments of shoreline position, rate of change, and factors contributing to shoreline change give citizens, organizations, planners, and regulators an indication of expected future change and help determine whether those changes are accelerating, decelerating, or continuing at the same rate as past changes.

Historical change rates of the South Texas gulf shoreline were first determined by the Bureau of Economic Geology (Bureau) in the 1970s and presented in a series of publications separated at natural boundaries along the approximately 530 km of shoreline (Morton and Pieper, 1975; Morton, 1977). This publication series presented net long-term change rates determined from shoreline positions documented on 1850 to 1882 topographic charts published by the U.S. Coast and Geodetic Survey (Shalowitz, 1964) and aerial photographs acquired between about 1930 and 1975. Rates of change for the entire Gulf shoreline were updated through 1982 on the basis of aerial photographs (Paine and Morton, 1989; Morton and Paine, 1990). Lidar-derived shoreline positions in 2000–2001 were used as part of a Gulf-wide assessment of shoreline change that included the Texas coast (Morton and others, 2004, 2005). Coast-wide rates of historical shoreline change were recently updated using 2007 aerial photographs, the most recent coast-wide coverage predating Hurricane Ike in 2008 (Paine and others, 2011, 2012). Through all of these studies, Bureau researchers have documented that the Gulf of Mexico shoreline along the middle and lower Texas coast is eroding at an average rate of about 1 m/yr.

This report presents and discusses short-term, decadal scale, and long-term shoreline change; geomorphic unit mapping; and beach-dune system volumetric analysis of South Padre Island and Brazos Island, Texas, determined from an airborne lidar survey conducted by the Bureau in February 2013. The survey mapped a swath of shoreline about 500 meters wide along the shoreline between Mansfield Channel and the Rio Grande. High-resolution color-infrared aerial photography was captured simultaneously. Utilizing the Bureau's Chiroptera aerial mapping system, bathymetric lidar was captured for a swath 1000 meters wide. Bathymetric lidar represents a fundamental advance in our ability to acquire nearshore data, but the Chiroptera was untested under murky-water conditions typical of the Texas coast. This project represented our first opportunity to establish the depth capability and water-clarity limitations of the system in Texas coastal waters.

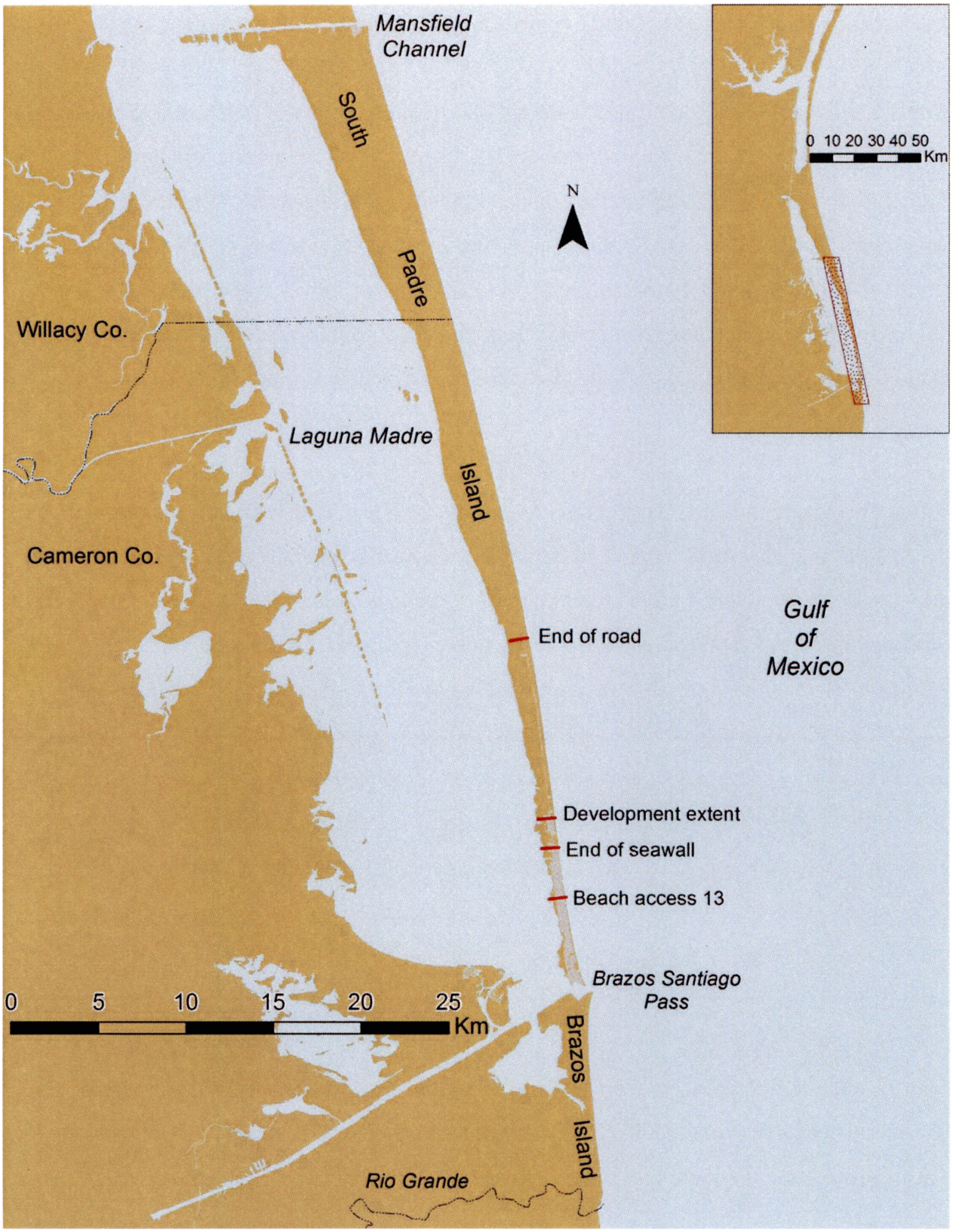

Figure 1. Index map of study area.

METHODS

Principal project tasks included (1) acquiring airborne topographic and bathymetric lidar data along South Padre Island and Brazos Island; (2) processing the topographic and bathymetric lidar data to produce full-resolution point clouds and a digital elevation model (DEM); (3) processing the CIR imagery to produce a ortho-rectified and mosaicked image of the study area; (4) extracting a shoreline from the DEM to analyze short-and long-term shoreline change; (5) mapping the potential vegetation line, back-dune line, geomorphic units, and maximum dune crest; and (6) extracting volume statistics to analyze volumetric change.

Data Acquisition

Researchers from the Bureau of Economic Geology (BEG) acquired lidar data and color infrared (CIR) aerial imagery of South Padre Island and Brazos Island, Texas, (Mansfield Channel to Rio Grande) on February 4 and 5, 2013. Data were collected using the BEG's new airborne system (Chiroptera, by Airborne Hydrography AB), which collects topographic lidar data, shallow bathymetric lidar data, and natural color/color infrared imagery. Topographic data and CIR images were collected for a 500-m swath (three passes) of South Padre Island and Brazos Island (71 km total length) landward of the shoreline. Bathymetric data were collected from the shoreline 1000 m seaward. A few transects were also flown across the Island and Laguna Madre, capturing both topographic and bathymetric data. This project is intended to establish the depth-penetration and water-clarity limitations of Chiroptera on the open Gulf of Mexico coast.

The Chiroptera topographic lidar scanner operates at a wavelength of 1 µm, a pulse rate as high as 400 kHz, and an incident angle (from vertical) of 28 to 40 degrees. It can operate to a maximum height of about 1,500 m, allowing the system to be used to scan large areas rapidly with a range accuracy of about 2 cm over a flat target. The bathymetric lidar scanner operates at a shorter wavelength (0.515 µm) and a lower pulse rate (36 kHz). The shorter wavelength allows the laser to penetrate water of reasonable clarity. After the laser reflects off the bottom

surface and back to the source, the transit-time delay between water surface and water-bottom reflections can be used to determine water depths to a flat-bottom accuracy of about 15 cm. Also mounted in the Chiroptera chassis is a Hasselblad DigiCAM 50 megapixel natural color (RGB) or color infrared (CIR) camera that acquires frame images at a resolution of 8,176 by 6,132 pixels.

The BEG aerial surveying capability has been augmented with the construction of "Goliath," a fast and secure mobile data-storage and processing system. Its two 40-terabyte (TB) RAID 5 arrays speed the transfer of field data by a factor of 10 over conventional storage systems while providing full redundancy to ensure data integrity. Goliath was designed and assembled to meet specific requirements of the Chiroptera lidar instrument and imaging system. Operating simultaneously, these components generate high-resolution data at the rate of about 1.5 TB per 2-hour flight. Goliath has been ruggedized for transport and field deployment and enables the research team to remain in the field for the duration of the project—sometimes as long as a week or more. More importantly, the new system allows researchers to visualize and verify the quality of collected data each field day, ensuring adequate areal coverage and optimal data quality.

For the South Padre Island survey, the Chiroptera was installed in a single-engine Cessna Stationaire 206 aircraft (tail number N147TX) owned and operated by the Texas Department of Transportation, and operated locally out of Harlingen, Texas. Flight elevation was 650 meters for the topographic survey and imagery capture of South Padre Island and Brazos Island. Topographic laser pulse rate was 200 kHz. Flight elevation was 400 meters above sea level during the bathymetric survey offshore of South Padre Island and Brazos Island. The bathymetric laser was operated at the system maximum pulse rate of 36 kHz. The pilot followed the flight altitude, speed, and flight lines directed by the flight plan during each segment of the survey. High-resolution aerial images were collected using the integrated medium-format camera, and VGA low-resolution images were collected for the operator to reference during the survey and to aid post-processing. GPS and attitude (INS) information was

acquired along with lidar data and imagery to enable accurate georeferencing. The survey was completed in three flights over two days (fig. 2). The February 4, 2013, flight included three land passes along South Padre Island. This flight also included transects along the Mansfield Channel, across a rookery island adjacent to Mansfield Channel, and through Brazos Santiago Pass. The two flights on February 5, 2013, included three land passes along Brazos Island, all bathymetric passes (seven or eight offshore passes between Mansfield Channel and the Rio Grande), and two transect passes perpendicular to South Padre Island. Two GPS base stations, set for continuous 1-second data-collection rate, were operated during the survey at Port Mansfield and the South Padre Island Convention Center.

Lidar Data Processing

All laser data, raw image files, and positional data were downloaded to the field computer. Preliminary GPS processing is completed by merging base GPS receiver data with the remote (aircraft GPS) data to create a GPS trajectory. The preliminary GPS trajectory is combined with attitude information to create a seven-parameter (time, X, Y, Z, roll, pitch, yaw) navigation file. The navigation solution is used to reference each laser pulse return with the seven-parameter information in LSS. Laser-point-cloud data are output by flight line in multiple segments. Point-cloud data is examined to determine quality of the data coverage (i.e., sufficient overlap of flight lines and point spacing).

Upon return from the survey area, all files are transferred from the field computer to an in-house server. Base-station coordinates are computed using National Geodetic Survey's (NGS) Online Positioning User Service (OPUS). A project is set up using AEROoffice software to covert Chiroptera GPS files to a binary Novatel GPS file. The aircraft GPS file and base station GPS files are then converted to a GrafNav compatible format. A merged aircraft trajectory is computed using GrafNav software. Solutions for base-station coordinates and aircraft trajectories are in the NAD83 (2011). The aircraft trajectories are converted to the WGS84 datum when output from GrafNav. The precise trajectories are combined with aircraft attitude information in AEROoffice to create a final precise seven-parameter navigation file.

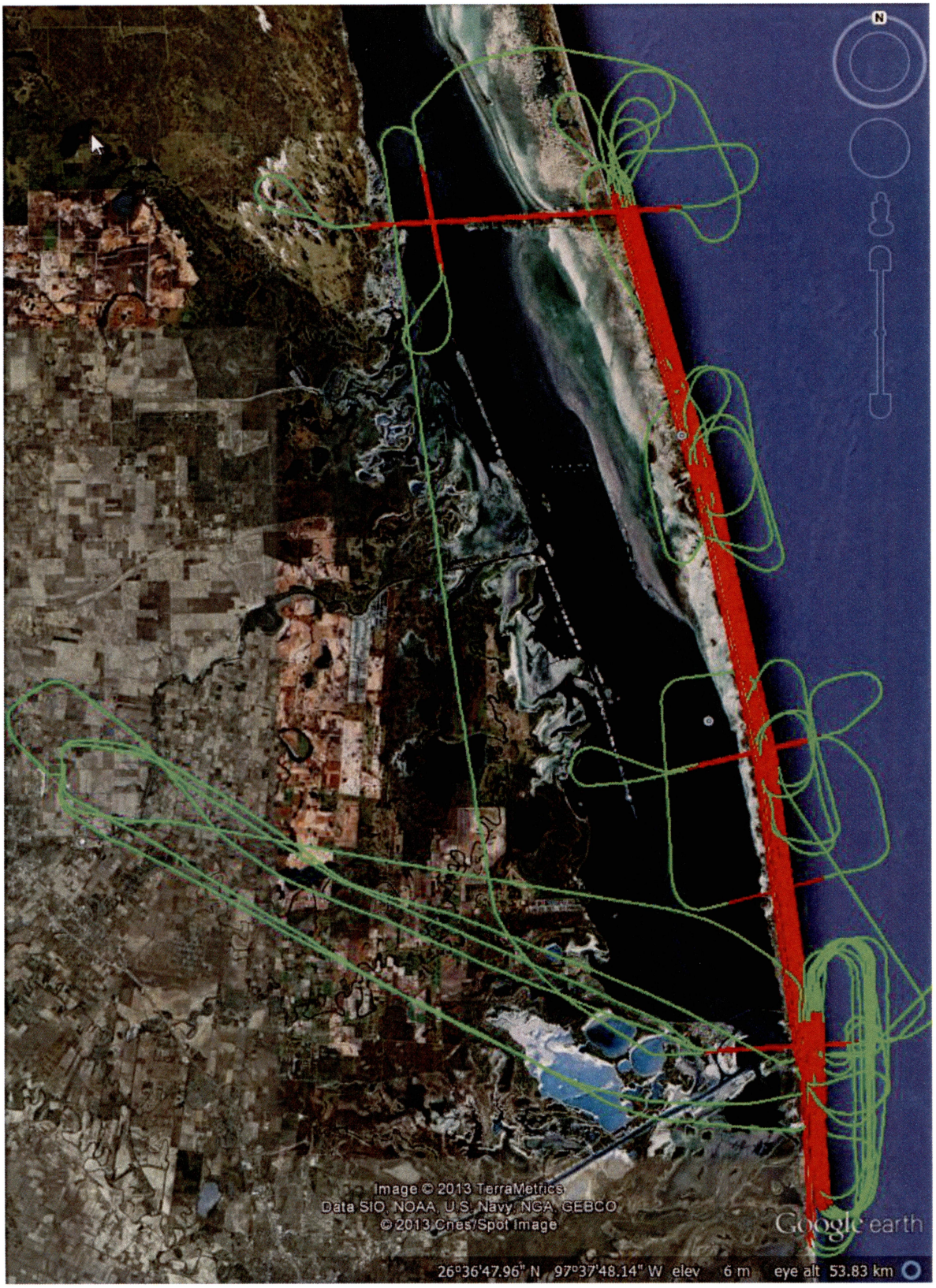

Figure 2. Trajectories of all three flights, showing coverage between Mansfield Channel and Rio Grande. Red segments indicate when lasers were firing.

Topographic Processing

Laser-point data are generated in AHAB processing software Lidar Survey Studio (LSS), combining navigation file information and laser data. LSS also requires calibration, processing settings, and system- configuration files. Laser-point data is output from LSS in LAS v1.2 format (a binary file format). A condition is set in LSS to output data in the proper UTM zone and hemisphere. The resultant points are referenced to the Geographic WGS84 horizontal datum and height above the WGS84 ellipsoid. The TerraScan utility of MicroStation was used to concatenate flight line files, combine flight lines and decimate data into USGS quarter quadrangles, determine bias offsets between lidar point data and kinematic GPS ground reference control points, and clean the data of miscellaneous returns (such as clouds, reflections, and long returns). Ground GPS surveys were conducted within the lidar survey area to acquire ground-truth information. The ground survey points are estimated to have a vertical accuracy of 0.01–0.05m. Roads or runways, which are open areas with an unambiguous surface, were surveyed using kinematic GPS techniques. A lidar data set was sorted to find data points that fell within 1 m of a ground GPS survey point. The mean elevation difference between the lidar and the ground GPS was used to estimate and remove an elevation bias from the lidar. The standard deviation of these elevation differences provides estimates of lidar precision. Vertical biases were determined for and removed from each flight. Average RMS for 20130204 is 0.0332m, 20130205A is 0.0448m, and 20130205B is 0.028m. The 2012A geoid model was used to adjust the elevation data from ellipsoidal to orthometric heights (NAVD88) using a LAStools script called lasheight. This script was also used to remove elevation bias between the laser-point data and ground control points. A DEM was generated from the input LAS files using the LAStools script lasgrid.

Bathymetric Processing

A separate calibration file for bathymetric data processing is prepared in order to align vertical elevation control points with laser-point-cloud data and to eliminate roll, pitch, and yaw errors caused by IMU misalignment. LSS parameters are adjusted to minimize noisy data output. A configuration file is prepared by setting amplitude thresholds and backscatter threshold values.

A water-refraction value based on salinity is computed to provide optimum performance (1.3435). The select map option is utilized to automatically determine the water surface elevation (within LSS). After initial processing, waveform information is analyzed to determine if the laser returns are being classified properly. Bathymetric laser-point data are output from LSS in LAS v1.2 format (a binary file format). Using the TerraScan utility of MicroStation, flight line segment files were concatenated, adjacent flightlines were combined, and Class 7 (bottom/seafloor) and Class 5 (water surface) are extracted as separate files.

Offshore transects collected by Naismith Marine Services, Inc., for HDR Engineering, Inc., the Texas General Land Office, and the City of South Padre Island in October 2012 were used as ground truth for the southern portion of study area. The transect data points were collected within the limits of the City of South Padre Island, a stretch of shoreline 10 km long and extending offshore approximately 1.4 km to water depths between 9 and 10 meters. The transect data points were used to verify the bathymetric points that were classified as bottom returns.

The 2012A geoid model was used to adjust the elevation data from ellipsoidal to orthometric heights (NAVD88) using the LAStools script lasheight. A bathymetric DEM (3-meter cell size) was generated from the input LAS files using the LAStools script lasgrid. The bathymetric grid was then resampled to 1-meter spacing and a smoothing algorithm was run over the new 1-meter DEM. The smoothed bathymetric grids were then merged with the topographic grids to create a seamless topographic and bathymetric DEM (fig. 3).

Aerial Imagery Post-Processing

High-resolution aerial photography was collected simultaneously during the lidar survey. Post-processing of the imagery uses the same GPS and attitude (INS) information collected for the lidar survey. After the survey flight, the raw image files are downloaded to the field computer. Upon return from South Padre Island, all files were transferred from the field computer to an in-house server. Base-station coordinates were computed using National Geodetic Survey's

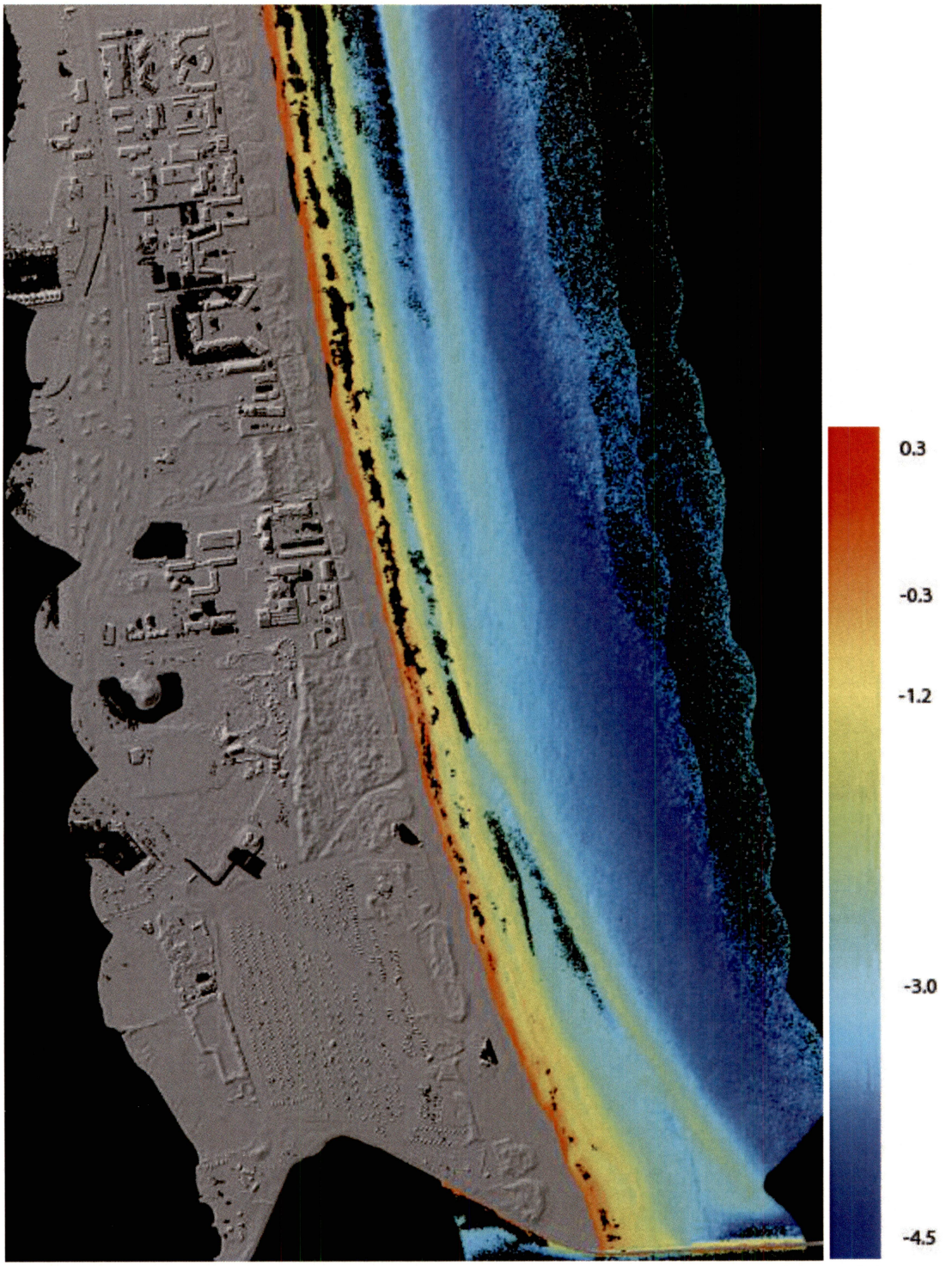

Figure 3. Merged topographic and bathymetric digital elevation model (DEM) for area north of Brazos Santiago Pass. Topographic DEM illustrated as shaded relief map. Color scale for bathymetric DEM shown at right. Units in meters.

(NGS) Online Positioning User Service (OPUS). AEROoffice software was used to convert the raw Chiroptera GPS files to binary Novatel GPS files. The aircraft GPS file and base-station GPS files are then converted to GrafNav-compatible format. A merged aircraft trajectory is computed using GrafNav software. Solutions for base-station coordinates and aircraft trajectories are in the NAD83 (2011). Aircraft trajectory positions are converted to WGS84 datum when output from GrafNav. The precise trajectories are combined with aircraft attitude information in AEROoffice to create final precise seven-parameter navigation file.

Hasselblad's software, Phocus, was used to export 1886 images from native format to TIFF. During export, output TIFFs are corrected for lens distortion and vignetting. ImageMagick software was used to move/re-order channels and then isolate the IR return to a single channel:

IR from channel 3 to channel 1

Red from channel 1 to channel 2

Green from channel 2 to channel 3.

The images were then brought into TerraPhoto for orthorectification and seam removal. The result created 27 one-meter resolution, 4000 x 4000 m tiles exported in ECW format. The ECW files were opened in ERMapper, color-balanced, and saved as a single 1-meter geoTIFF mosaic. The 1-meter geoTIFF was opened in Photoshop and color-matched to existing CIR imagery.

GIS Data Deliverables

Several data products were extracted from the lidar DEM and photography and delivered as ArcGIS shapefiles and GoogleEarth KMZ files.

Shoreline

Prior to using lidar to map the shoreline feature, vertical aerial photography was used. Shorelines were drawn or digitized on the photography by using the boundary between wet and dry sand on the beach. The position of this boundary varied due to water level conditions, wave activity, and errors in geo-referencing the photography. Through analysis of lidar surveys

and repeated beach profiles, Gibeaut and others (2002) and Gibeaut and Caudle (2009) determined that the wet/dry boundary occurs 0.6 m above local mean sea level. Using the seaward-most, continuous contour of 0.6 m above local mean sea level provided a consistent shoreline feature between lidar datasets.

When lidar data are processed, the elevation values are reported in height above an ellipsoid (HAE). These values are then transformed to North American Vertical Datum of 1988 (NAVD88) orthometric height by applying a geoid model correction. Previous BEG-acquired lidar datasets (2000–2012) used the National Geodetic Survey's (NGS) GEOID99 model to make the transformation between ellipsoidal heights to NAVD88 heights. A mean sea-level correction was also applied before extracting the shoreline from the lidar datasets. GEOID99 has been superseded by new iterations of geoid models. The NGS produces new geoid models every few years to more accurately represent the current Earth surface and incorporate additional data. GEOID12A was released by the NGS in September 2012. Current BEG lidar datasets use the GEOID12A model to transform between ellipsoidal heights and NAVD88 orthometric heights. The NAVD88 heights calculated with GEOID12A are higher than the heights calculated with GEOID99; therefore a new shoreline elevation needed to be determined. Through analysis of the most recent beach profiles and aerial photography, the 1.05-meter above NAVD88 (GEOID12A) contour was selected as the shoreline position on the February 2013 lidar DEM.

The delivered shapefile mapped the February 2013 shoreline (fig. 4) on the Texas Gulf coast between Mansfield Channel and the Rio Grande (South Padre Island and Brazos Island). The 1.05-meter elevation contour was selected from the DEM using the contour function in ArcGIS. The extracted file is then smoothed in ArcMap using the "Smooth Line" function (PAEK algorithm with a 2-meter smoothing tolerance). The number of vertices in the polyline is reduced by using ET GeoWizards "Generalize Polyline" command with a 0.25 m tolerance. This process retains the shape of the smoothed polyline while reducing the number of vertices. Topology errors, including dangles, self-overlapping lines, and self-intersecting lines, were removed. Adjacent line segments were aggregated using ArcGIS's "Unsplit Line" function.

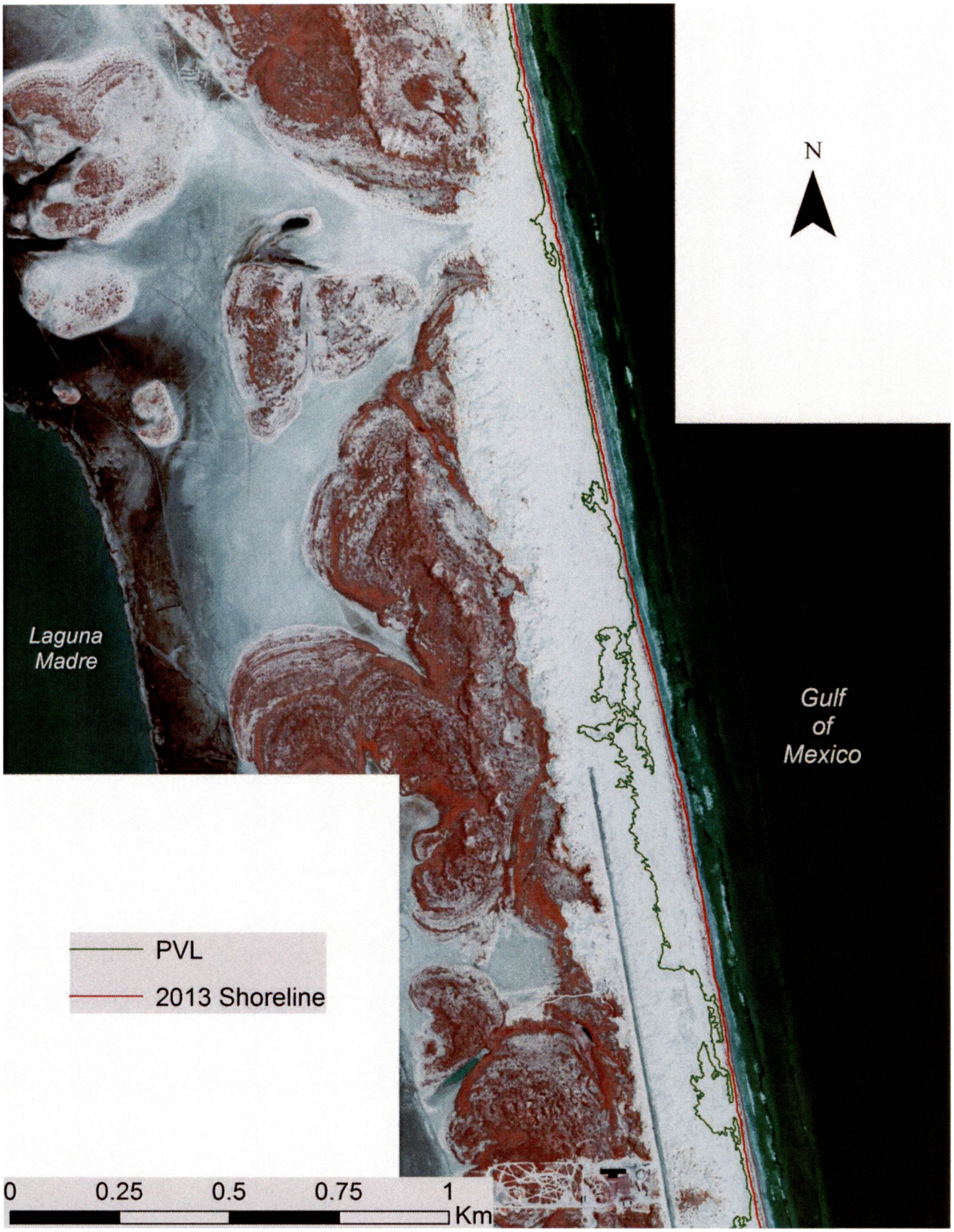

Figure 4. 2013 shoreline and potential vegetation line positions on South Padre Island.

Potential Vegetation Line

Mapping the natural line of vegetation has proven difficult when establishing a legal boundary for the Texas Open Beaches Act (OBA). Gibeaut and Caudle (2009) sought to establish a consistent mapping technique based upon lidar elevation data that can be used to determine the "potential vegetation line" or PVL. Because of the difficulty in rigorously mapping the landward boundary of the public beach easement as the line of vegetation, Gibeaut and Caudle (2009) recommended that an elevation be selected that represents the lowest elevation at which foredune vegetation may form a continuous cover. The seaward-most contour line with an elevation of 1.50 m above NAVD88 (GEOID12A) is used as the boundary. This elevation was derived from statistical analysis of long-term beach profile elevation data of natural dunes along the Texas coast. The extracted line will either be within the vegetation or coincide with the vegetation line. Where it is seaward of the vegetation, it indicates the potential position to where vegetation and the foredune may advance.

The seaward boundary of the potential vegetation line is mapped as a contour line 1.5 meters above NAVD88 (GEOID12A) on February 2013 lidar DEMs (fig. 4). The 1.5-meter elevation contour was selected from the lidar DEM using the contour function in ArcGIS. The lidar data are referenced to the NAVD88 datum. The relatively continuous contour line along the back edge of the beach and seaward edge of the foredune is selected as the potential vegetation line. The extracted file is then smoothed in ArcMap using the "Smooth Line" function (PAEK algorithm with a 2-meter smoothing tolerance). The number of vertices in the polyline is reduced by using ET GeoWizards "Generalize Polyline" command with a 0.25-m tolerance. This retains the shape of the smoothed polyline while reducing the number of vertices. Topology errors were removed including dangles, self-overlapping lines, and self-intersecting lines. Adjacent line segments were aggregated using ArcGIS "Unsplit Line" function.

Landward Dune Line

The position of the landward dune boundary, or back-dune line, is an important factor in determining the space required for dune formation, defining the dune complex for volumetric

and geomorphic analysis, and for use in determining design setback distances or creating dune restoration projects. An automated process for selecting the boundary is not effective because the landward dune boundary is based upon qualitative criteria that are interpreted by examining a combination of lidar data and aerial photography. Several criteria influence the selected position of the landward dune boundary. The boundary should (1) be at or near a change in slope from steep on the dune to gentle on the barrier flat; (2) have an elevation 2 m or more above mean sea level; (3) bound dunes that provide at least minimal storm-surge protection; (4) have an orientation that roughly parallels the shoreline; (5) be adjacent to the shoreline and features classified as dunes; and (6) connect adjacent forms classified as dunes (Gibeaut and Caudle, 2009).

The February 2013 landward dune boundary for the UTM Zone 14 Lower Texas Coast (Mansfield Channel to Rio Grande) was manually digitized at scales of 1:1,000 and 1:5,000 using February 2013 DEMs created from lidar data (fig. 5). The foredune complex was defined as the seaward-most continuous feature with an elevation of at least 2 m. If a single continuous feature is not present, dune clusters are considered as part of the complex as long as they are arranged quasi-parallel to the shore and are close together and/or connected. In areas where dunes are not present (e.g., washover areas), the dune boundary is mapped as the landward contour equivalent to the height of the potential vegetation line (1.5 m). A raster file representing the aspect of the DEM was used to help interpret the extent of the dune boundary by visualizing the landward slope of dune features. In addition, aerial imagery was used to locate the extent of vegetation and to help identify manmade structures. Manmade structures are not considered to be part of the foredune complex. The dune boundary is placed seaward of buildings or seawalls.

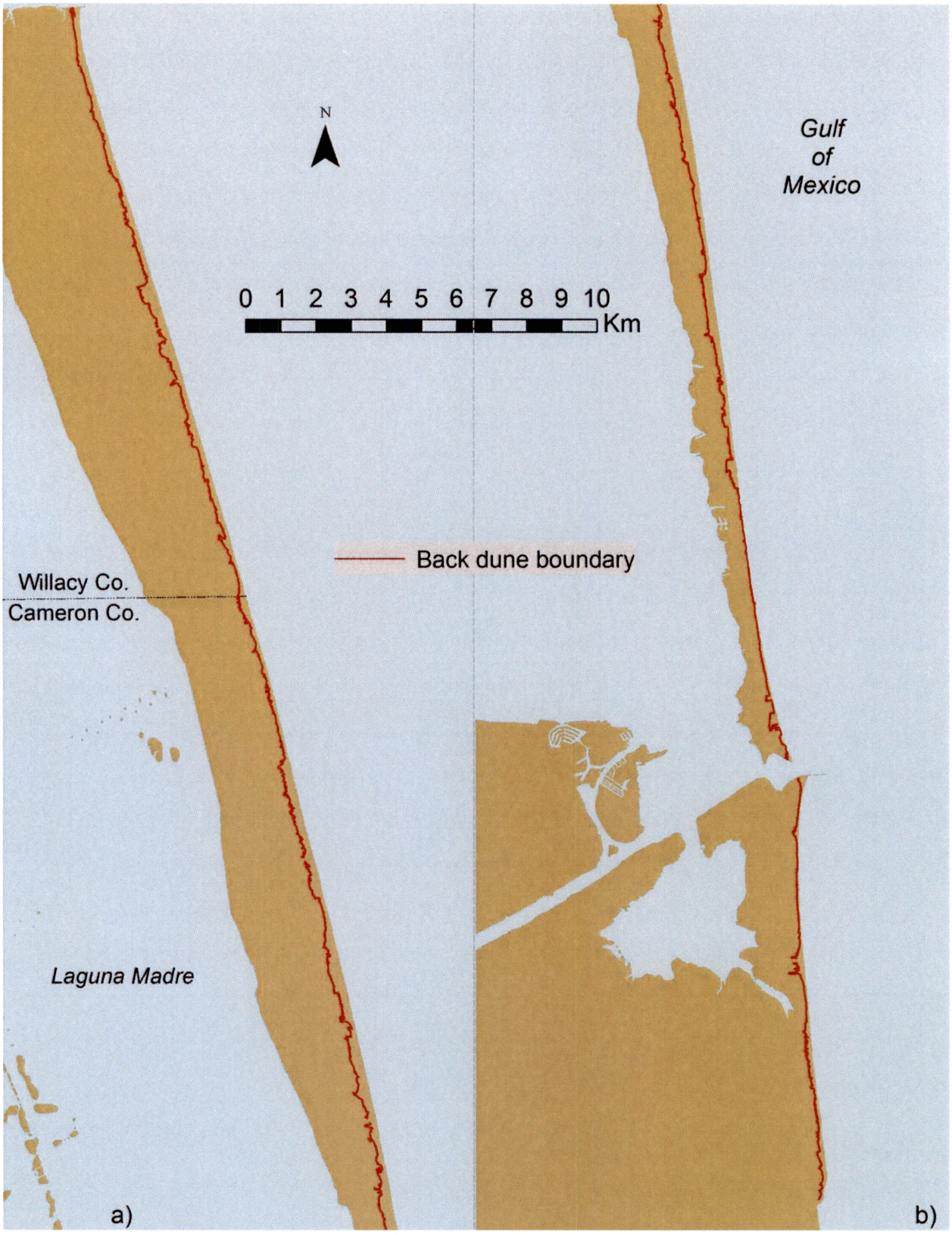

Figure 5. Location of landward dune boundary in (a) north and (b) south sections of study area.

Long-Term Shoreline Change Rates

Long-term shoreline change rates were calculated by including the 2013 South Padre Island shoreline into the set of shoreline positions that had been used previously to determine long-term Texas Gulf shoreline change rates presented in the Bureau's shoreline change publication series. Shoreline positions from the 1930's to 1990 were interpreted by mapping the wet beach/dry beach boundary from vertical aerial photographs and then optically transferred to U.S. Geological Survey 7.5-minute paper topographic base maps. These shoreline positions were digitized from the paper maps into an ArcGIS format. The 1995 shoreline was digitized as the wet/dry boundary directly from ortho-rectified digital aerial imagery. The 2000 shoreline was surveyed using an Optech ALTM 1225 lidar instrument. Shoreline position was extracted from the lidar-derived digital elevation model at 0.6 meters above mean sea level (calculated from Geoid99). The 2007 shoreline was mapped digitally within a GIS by digitizing the wet beach/dry beach boundary as depicted on high-resolution, geo-referenced aerial photographs taken in September and October 2007. The positions of likely stationary natural features and infrastructure shown on 2007 photographs were compared to the positions of correlative features on geo-referenced 2010 aerial photographs to ensure accurate positioning. The 2013 shoreline position was extracted from the lidar-derived digital elevation model at 1.05 meters above NAVD88 (Geoid12A).

Shorelines were selected for the change-rate analysis to conform to shorelines chosen for earlier calculations of shoreline change rate and to give regular intervals between shorelines along a given transect. The included shorelines for the long-term change-rate calculation were from 1937, 1960, 1974, 1975, 1995, 2000, and 2013 (fig. 6). Shorelines from 2010, 2011, and 2012 were included for a short-term shoreline-change analysis. The software DSAS (Digital Shoreline Analysis System; Thieler and others, 2009) was installed on ArcGIS 10.1 to facilitate calculation and GIS-based analysis of shoreline change. A shore-parallel baseline was created from which DSAS cast shore-perpendicular transects at 50-m intervals along the shoreline. The DSAS extension was then used to calculate long-term rates of change and associated statistics using the transect location and the selected shorelines (fig. 7). A GIS shapefile was then created

that contains the intersection point of the 2013 shoreline with the shore-perpendicular transect lines and the following statistics:

- End-Point Rate (in meters per year), the calculated rate of change determined from the earliest and most recent shoreline position, averaged over the elapsed time.
- Shoreline-Change Envelope (in meters), the total distance between the shoreline farthest from and closest to the baseline at each transect.
- Net Shoreline Movement (in meters), the total distance between the earliest and latest shoreline position. Negative values indicate shoreline retreat.
- Linear Regression Rate (in meters per year), the rate of shoreline change calculated from all shoreline positions along the transect using the linear regression method.

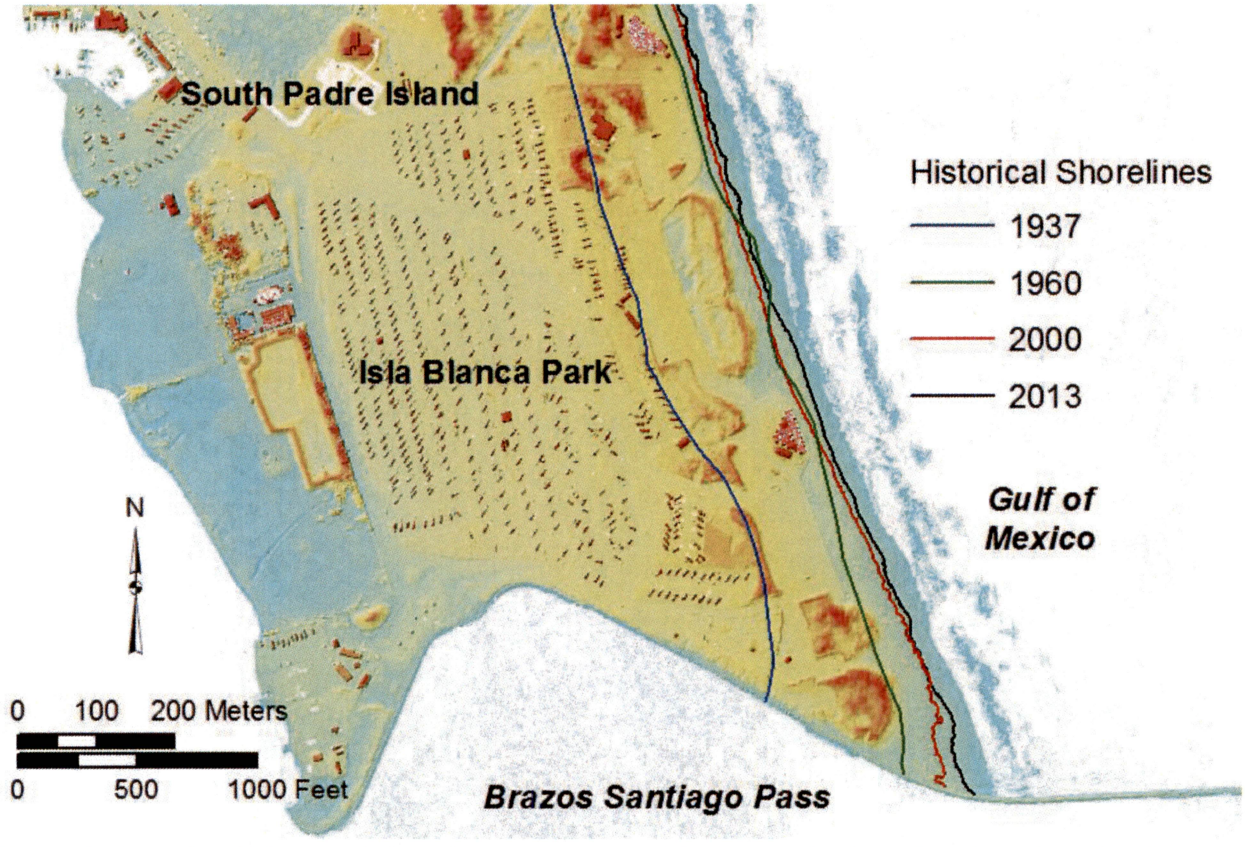

Figure 6. Sample of historical shoreline positions at Isla Blanca Park on South Padre Island.

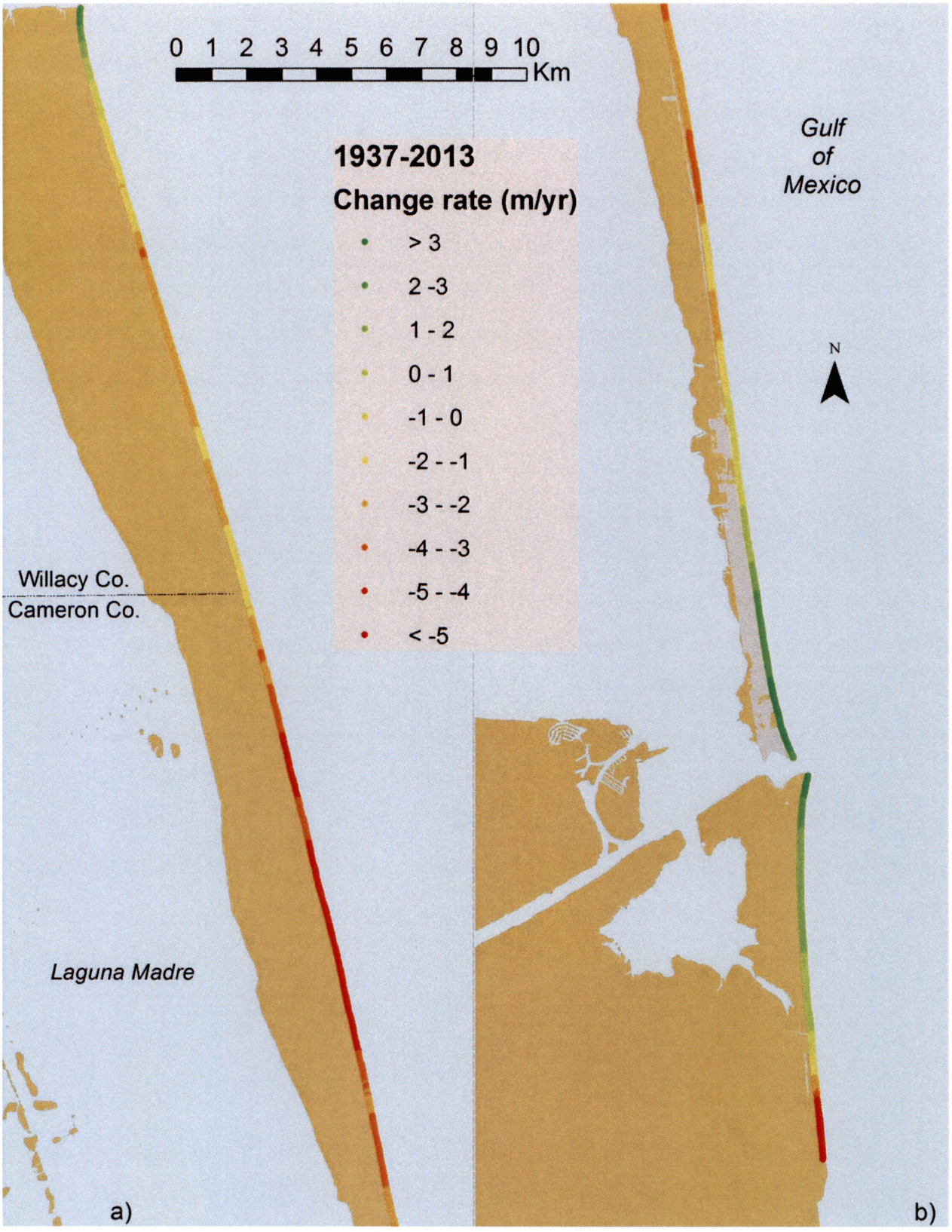

Figure 7. Long-term change rates in (a) north and (b) south sections of study area.

Geomorphic Units

Geomorphic units along South Padre Island were manually mapped at a scale of 1:5,000 by combining CIR aerial imagery and topographic lidar data (figs. 8 and 9). The geomorphic classification system is a combination of classification systems derived for previous mapping exercises in similar barrier island environments and the National Wetlands Inventory (NWI) system of Cowardin and others (1979). Wetlands habitats are interpreted from BEG-captured 2013 CIR aerial imagery and follow the NWI classification scheme. Upland geomorphic units are mapped from the CIR imagery and a contemporaneously collected lidar dataset. Lidar data are processed, corrected, and converted to GIS-compatible files. Visualization techniques, some developed at BEG, were applied to the DEM for mapping purposes. Dune boundaries were mapped with the aid of a slope map that accentuated the toe of the dune. The primary mapping medium is the aerial image. However, the DEM proved to be a significant aid to geomorphologic mapping. A previous wetlands status and trends study mapped wetlands on South Padre Island on the basis of 2002 National Agriculture Imagery Program (NAIP) data. The 2002 mapping formed the base from which recent wetland boundaries were captured. Recent wetland mapping serves as the non-upland component of the geomorphic map. Newly distributed 2012 NAIP photography was used as ancillary information for upland geomorphic units and wetlands mapping. As part of an earlier mapping effort, washover features were interpreted from early 1990's aerial videography and photography. Washover channels and fans are two of several upland geomorphic units. Other units include fore-island dune complex, fore-island dune ridge, vegetated barrier flat, mid-island dune complex, and back-island dune complex, among others.

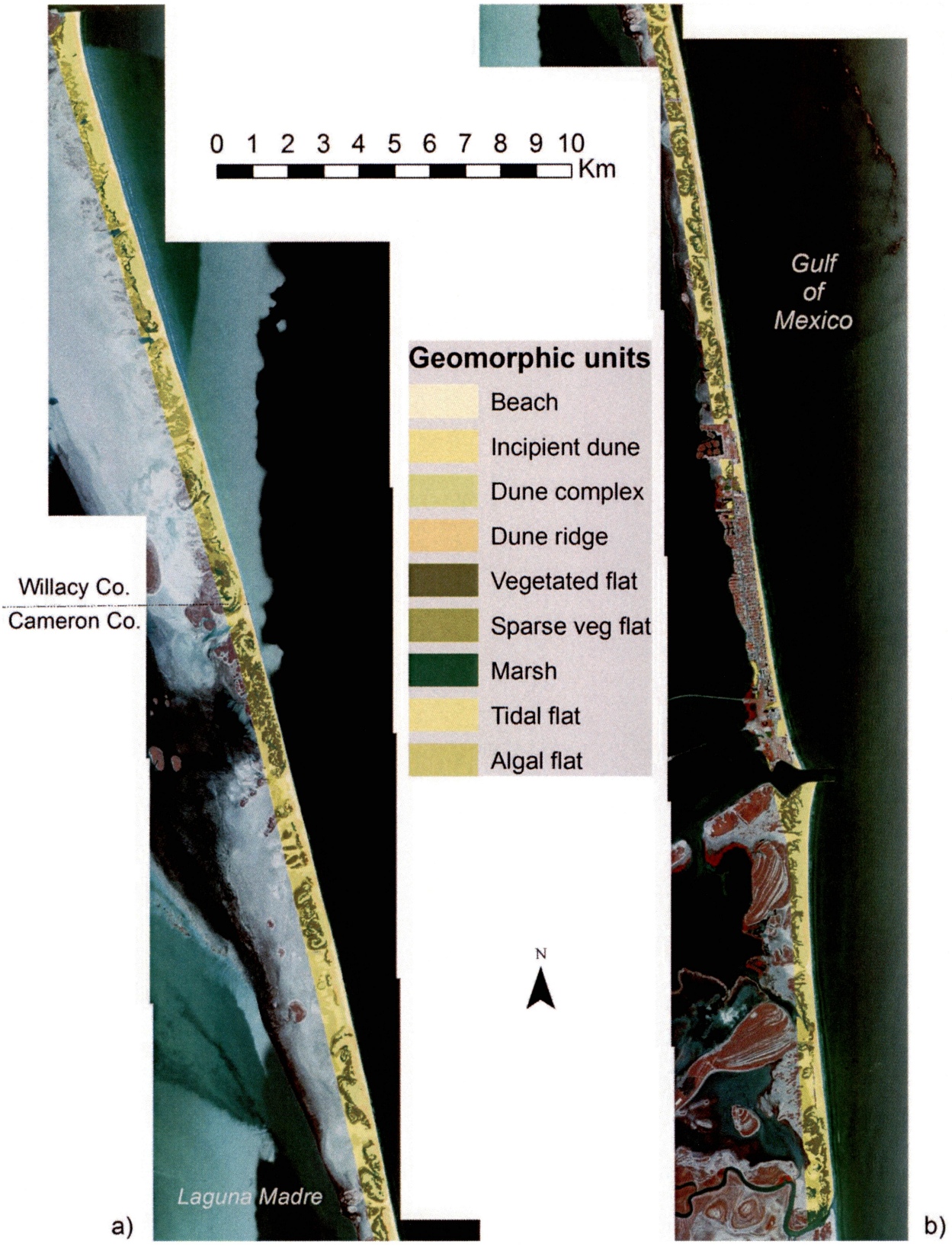

Figure 8. Geomorphic units within (a) north and (b) south sections of study area.

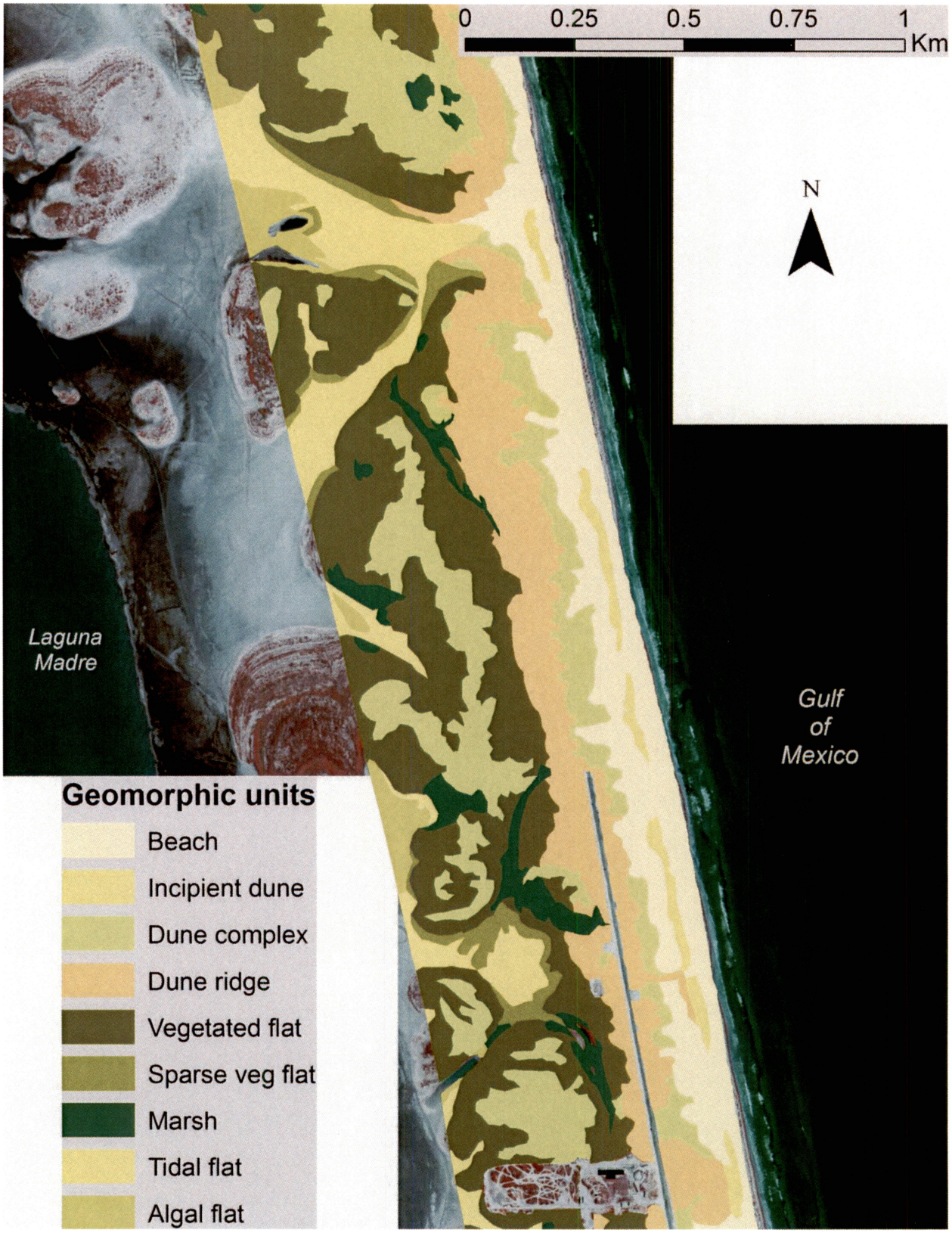

Figure 9. First appearance of incipient dunes north of Brazos Santiago Pass. Beach modification south of this point prohibits formation of incipient dunes.

Maximum Dune Crest Position and Volume Statistics

Evaluating the maximum dune-crest height and the volume of sediment in the beach and dune system helps scientists and decision makers understand beach and dune morphodynamics. Manual digitization of the position of the foredune crest is both time consuming and based on an individual's interpretation of a DEM. We decided to extract the highest crest elevation (over 2 m) along transects perpendicular to the South Padre Island and Brazos Island shoreline, using a spacing of 5 meters. A program (shorestat) was written to open a DEM and the shoreline file to extract this information. Shorestat also simultaneously calculates sand volume in the beach and dune system along each transect.

The 2013 shoreline and landward dune line shapefiles for South Padre Island and Brazos Island were merged and converted into a polygon file. The polygon file was then used to clip the full dataset DEM. This step creates a dataset that represents the beach and dune system only. The shoreline shapefile was exported to a simple ASCII text file. Shorestat opens the clipped DEM and the shoreline text file to extract the dune crest position and height as well as the sand volume in the beach and dune system.

Using the shoreline text file, shorestat generates a pseudo-shoreline x-y coordinate set along the shoreline at 5-m spacing. Transects perpendicular to the actual shoreline file would complicate dune-crest extraction and volume calculations—in many places, adjacent transects would not be sufficiently parallel to each other. A pseudo-shoreline is generated by averaging the shoreline deviation from true north up and down the coast and then generating new points at 5-meter intervals using the nearest average angle deviation from true north.

The program calculates shore-perpendicular transects using the angle calculated above plus 90 degrees at each pseudo-shoreline coordinate. The program traverses each transect at 1-m intervals, (a) seeking the highest point along transect and (b) calculating sand volumes at each 1-m-interval location. Shorestat extracts all the z-values from the DEM along each transect, selecting the highest elevation point along with its x-y position (fig. 10). Sand volume is

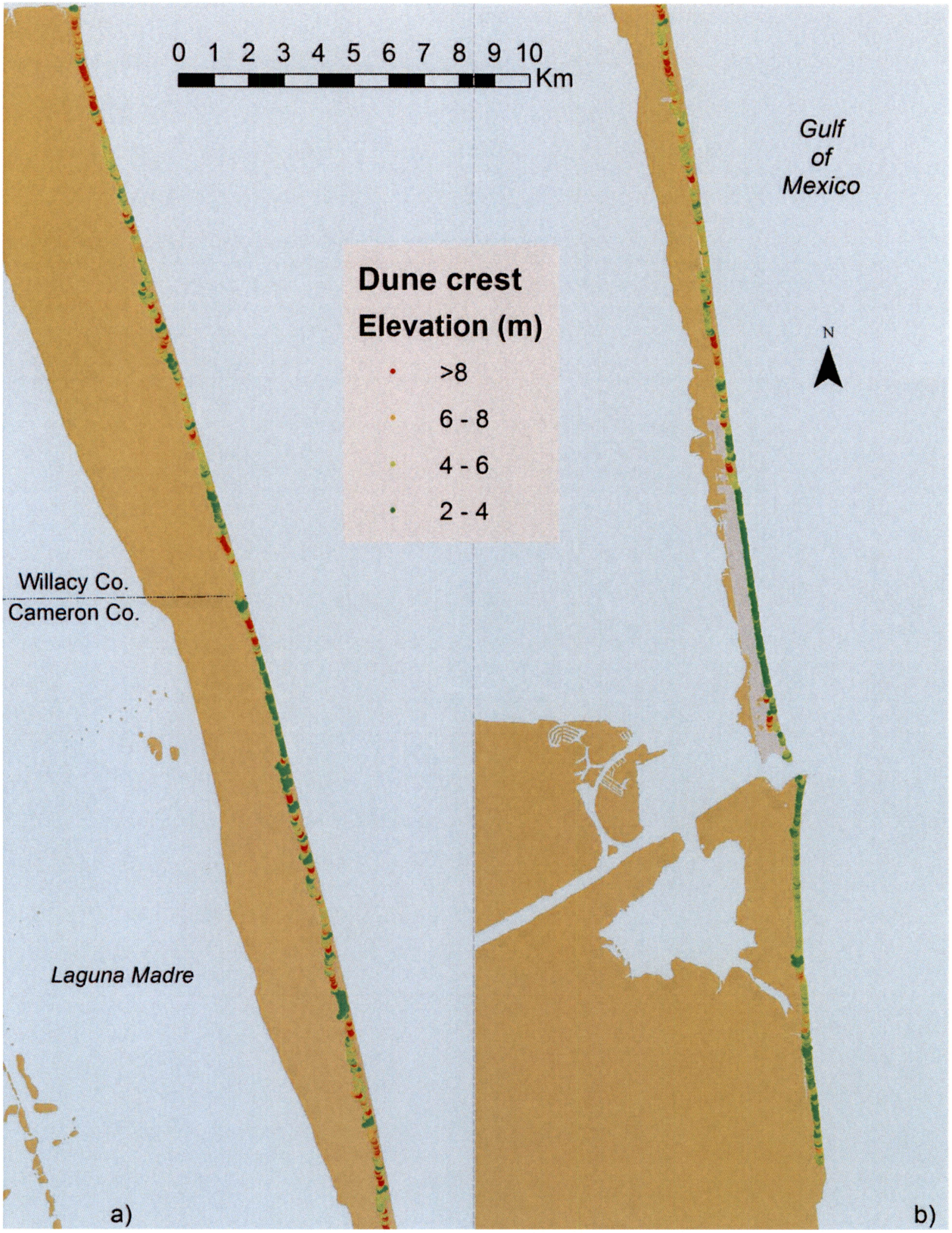

Figure 10. Maximum dune crest elevations along (a) north and (b) south sections of study area.

calculated above six threshold elevations starting at 1 meter above NAVD88. Volume is also presented as a percentage of total sand above each elevation threshold. All of the sand in the beach and dune system is above 1 meter NAVD88; therefore that column represents 100%. After completion of the calculations, shorestat writes four output text files: all_stats.txt, dunecr.txt, volume.txt, and trans.txt. The text files were then loaded into Global Mapper and exported to ArcGIS shapefile format.

BARRIER ISLAND GEOMORPHOLOGY

Prominent features on South Padre Island and Brazos Island are shown in the profile in Figure 11. Not shown are the numerous hurricane washover channels (fig. 12) through which surge waters flow, scouring channels and depositing sediments in washover fans on the lagoonward tidal flats. Much of South Padre Island is considered a low-profile barrier island (White and others, 1978), and hence does not have a continuous, vegetated, stabilized fore-island dune ridge. The dry climate and storm washovers lead to vegetation fragmentation and blowouts that are the sources of active dunes that migrate landward (fig. 13). Left behind the migrating dunes are deflation flats and troughs—topographic lows in which higher moisture levels support marsh vegetation (fig. 14).

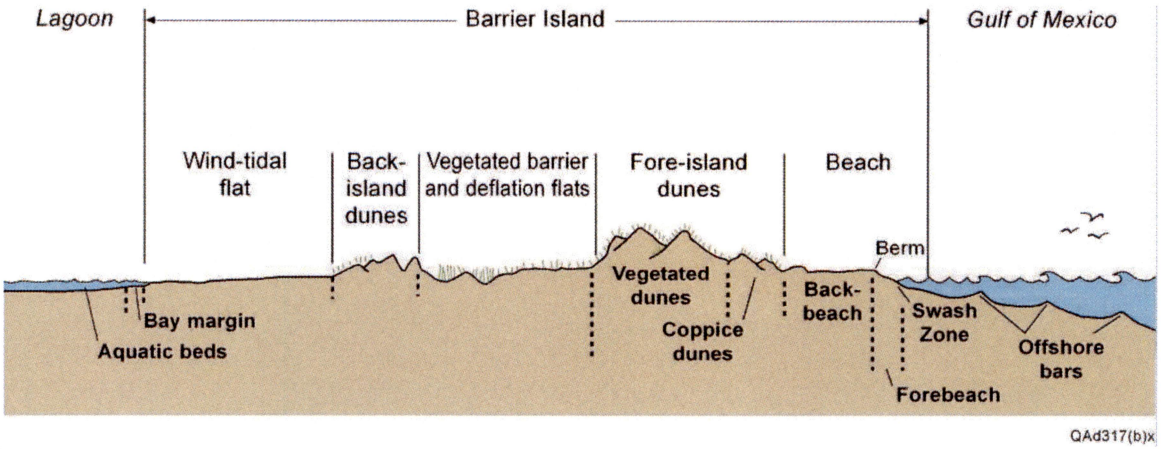

Figure 11. Generalized barrier island profile illustrating prominent features. From White and others (2005).

Figure 12. Storm washover channel.

Figure 13. Active dune and deflation area.

Figure 14. Marsh in depression lagoonward of fore-island dune ridge.

In this semi-arid climate, the most extensive habitats are broad wind-tidal flats (fig. 15). Astronomical tides on the Gulf shore are about 0.4 m and in lower Laguna Madre about 0.3 m. The range in tides caused by persistent winds, however, can be much higher than the astronomical tides, flooding much broader flats. The numerous storm washover channels that become active during hurricanes and tropical storms are closed between storms by sediments transported alongshore. The scoured channels pond water and support marshes along their margins (fig. 16).

Figure 15. Wind-tidal flats.

Figure 16. Marsh vegetation along margins of storm washover channel on South Padre Island.

The geomorphology map includes open water areas, the majority being marine open water. For analysis purposes, open-water areas mapped in this study are excluded. All other wetland and upland areas total 4,632 ha. The most abundant geomorphic unit in the study area is vegetated barrier flat. Flats are composed of heavily vegetated sand and shell. Many of the vegetated barrier flats are found on what Brown and others (1980) described as fan "islands" (fig. 17). Covering 904 ha (fig. 18), vegetated barrier flat is found throughout the non-developed barrier system in Cameron County and to a lesser degree in Willacy County. Vegetated barrier flats comprise 19% of the total terrestrial map area. Tidal flats were mapped in an earlier wetlands mapping effort and modified where appropriate. The second largest geomorphic unit, tidal flats cover 763 ha or 16% of the barrier system. High estuarine intertidal flats occur on the bay side of the island and beach on the Gulf side. While not a geomorphic unit, modified land ranks third in areal coverage at 543 ha or 12% of the mapped area. The fore-island dune ridge is a linear, shore-parallel, relatively high-relief feature adjacent to the beach in the fore-island area and includes some stabilized blowout dunes. Composed of vegetated and non-vegetated sand, the dune ridge covers 481 ha or 10% of the study area. Also in the fore-island area and in roughly the same amount (453 ha), the adjacent fore-island dune complex is comprised of relatively low-relief sand dunes and hummocks. The dune complex is mostly stable except in disturbed areas. The last dominant geomorphic unit is the sparsely vegetated barrier flat. The sand and shell flat is slightly less prevalent than the former units, at 397 ha or 9% of the map area. Mid-island dune complex (6%) and algal flat (5%) follow in acreage.

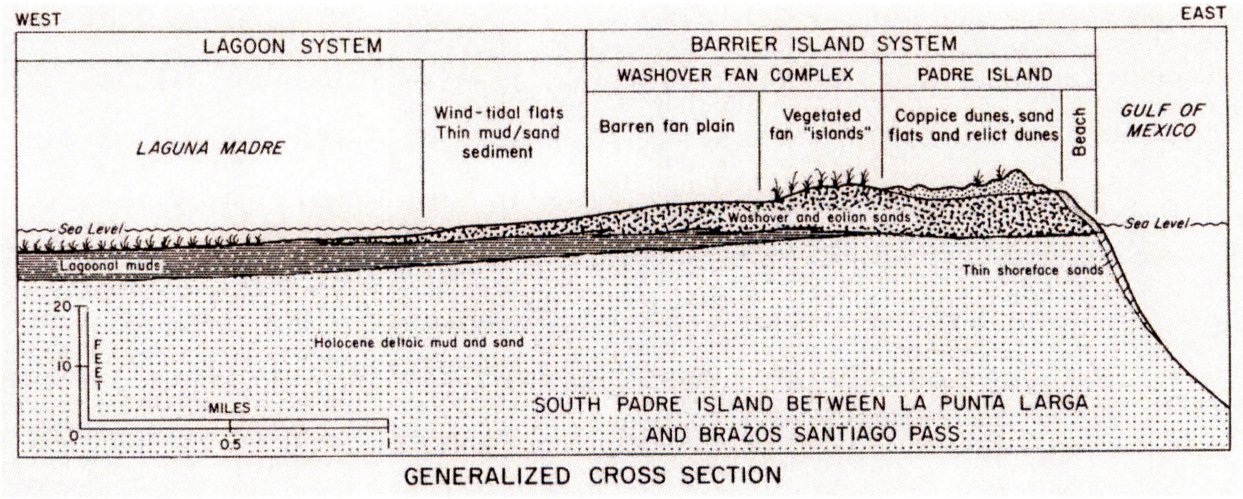

Figure 17. Generalized cross section of Padre Island barrier system. From Brown and others (1980).

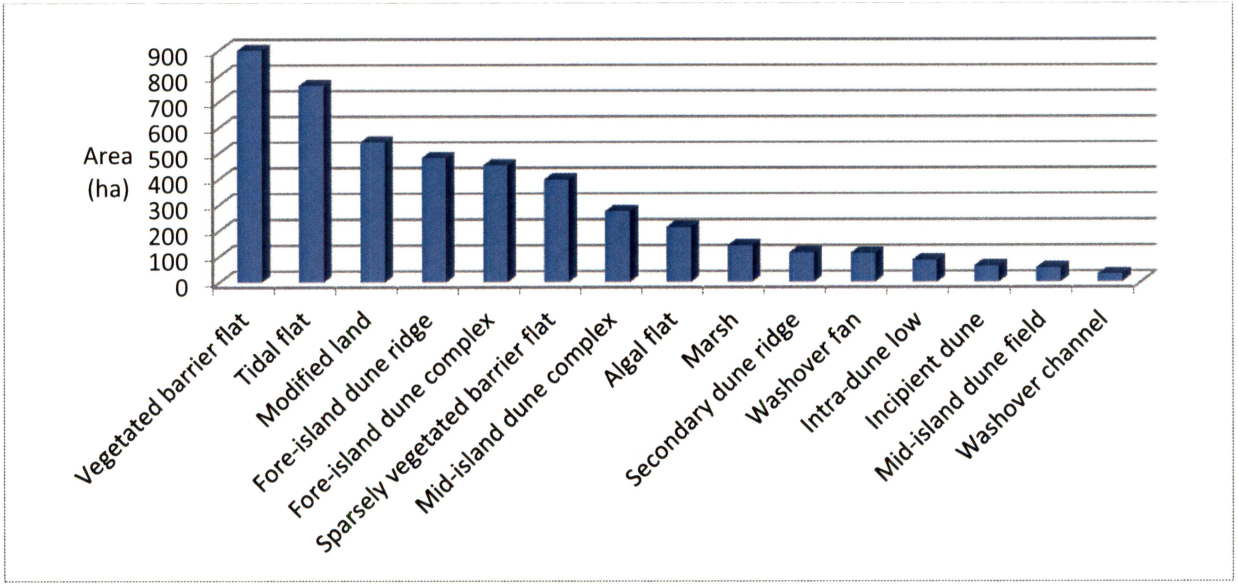

Figure 18. Geomorphic unit area in South Padre Island study area.

SHORELINE CHANGE

The principal natural geomorphic feature in this area is Padre Island, a long Holocene barrier island that broadens from a narrow peninsula at Brazos Santiago Pass to a broad, sandy barrier island having a well-developed dune system throughout most of its length. The Rio Grande enters the Gulf of Mexico within this segment and has created a large fluvial/deltaic headland that forms the southern boundary of a regional longshore current cell that is bounded on

the north by the Brazos/Colorado headland. The Rio Grande has a large drainage basin (471,900 km^2) that extends into Mexico, New Mexico, and Colorado, but dams constructed on the middle and lower parts of the basin in 1954 (Falcon) and 1969 (Amistad), combined with extensive irrigation use of Rio Grande water on the coastal plain, have reduced the amount of sediment delivered to the coast. Engineering structures that have affected shoreline position include (1) the jetties and associated ship channel at Brazos Santiago Pass, where the 13-m deep channel is flanked by jetties that reach 870 m (north jetty) and 490 m (south jetty) into the Gulf; and (2) the shallower Port Mansfield Channel and its 620-m (north) and 140-m (south) jetties that protect the 5-m deep channel.

On the basis of development, South Padre Island can be divided into four regions or segments (see fig. 1). The City of South Padre Island occupies the southernmost portion of the island (10 km) and is highly developed. The developed section of South Padre Island is separated into two sections. The southern 8 km has a seawall that limits the back dune boundary. The northernmost section of the city is an area of recent development without a seawall. State Park Road 100 (Padre Boulevard/Ocean Boulevard) continues north for an additional 10 km from the developed portion of South Padre Island. There has been no development (homes, condominiums, parks, etc.) in this segment but the road provides beach access points. The road is landward of the dune system but in areas of active dunes (sparse vegetation) sand has migrated across the road. Occasionally sand is removed from the road and used for small beach nourishment projects within the city. The northernmost 36 km of South Padre Island is undeveloped.

Long-Term Change, 1937–2013

Rates of long-term Gulf shoreline change for South Padre Island and Brazos Island, calculated from multiple shoreline positions between 1937 and 2013 (fig. 19), averaged 2.2 m/yr of retreat for both net rate and linear regression rate calculations. Rates were calculated at 1,343 sites spaced at 50 m between Mansfield Channel and the Rio Grande. Net retreat occurred at

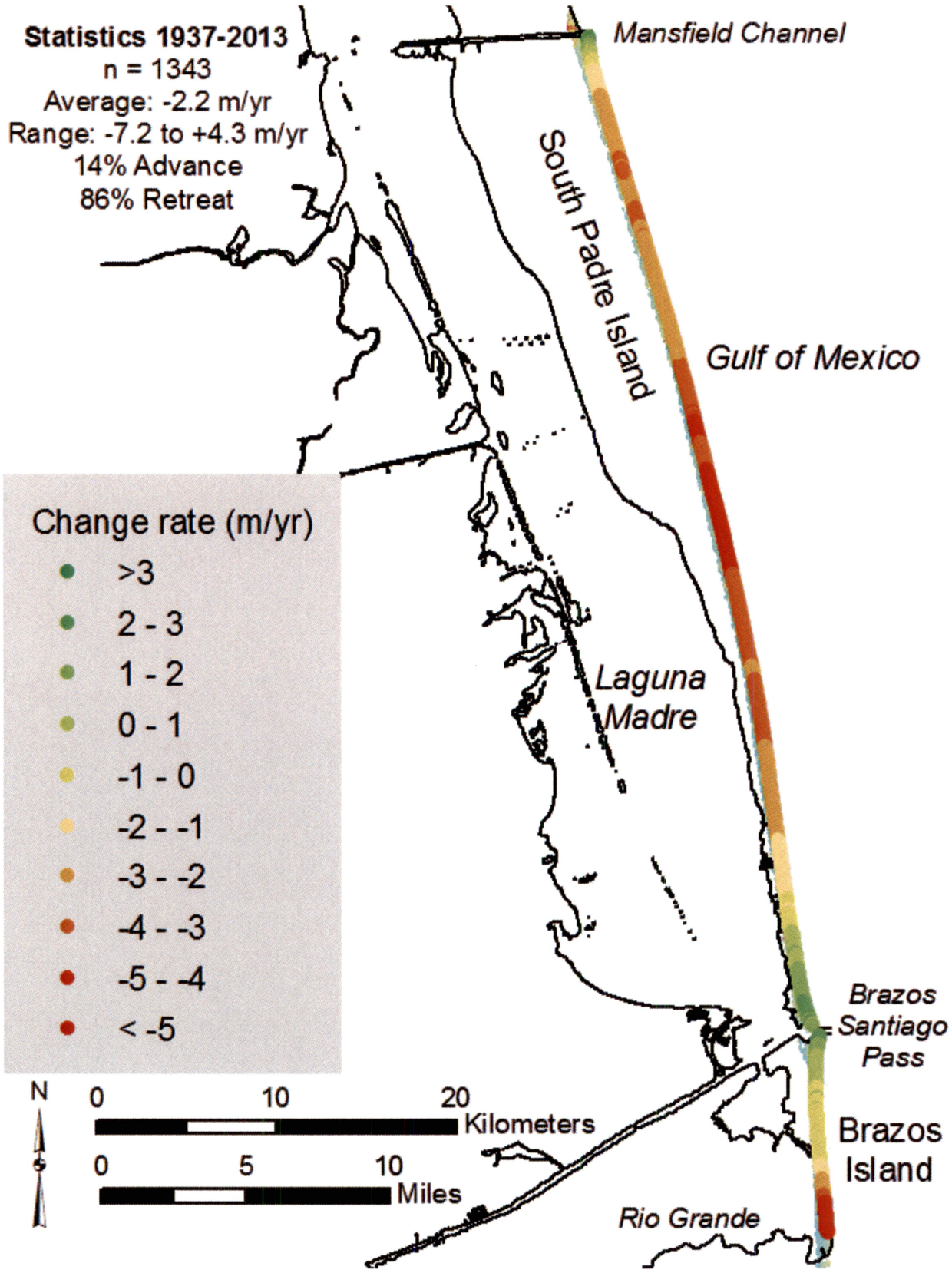

Figure 19. Net rates of long-term change for South Padre Island and Brazos Island calculated from shoreline positions from 1937 through 2013.

1,149 sites (86 percent) and advance occurred at 194 sites (14 percent) over the period of record. The overall rate is comparable to the average change rate (retreat at 2.3 m/yr) determined from the most recent previous update (through 2007; Paine and others, 2011).

Net change rates at individual sites ranged from advance at 4.4 m/yr to retreat at 7.2 m/yr. Net advancing shorelines include a 5.4-km segment adjacent to the north jetty at Brazos Santiago Pass, a 3-km segment adjacent to the south jetty at Brazos Santiago Pass, and a 1.3-km segment adjacent to the south jetty at Mansfield Channel. Net retreating shorelines include 49 km of South Padre Island and an 8-km segment north of Rio Grande (fig. 19). The highest net rates of shoreline retreat (greater than 3 m/yr) occurred along a 22-km segment in the middle of South Padre Island and a 2-km segment just north of the Rio Grande.

Brazos Island, between Brazos Santiago Pass and the Rio Grande, has an average net shoreline change rate of 1.2 m/yr of retreat (table 1). Retreat is occurring at 72 percent of sites on Brazos Island. The highest rates of retreat (7.2 m/yr) are found on Brazos Island in a small segment adjacent to the Rio Grande. The area protected by seawall experienced the least amount of average net shoreline change within the entire study area. The shoreline in this segment advanced at an average rate of 0.6 m/yr. The shoreline advanced at 67 percent of the sites along the seawall. The undeveloped area of South Padre Island (with and without State Park Road 100) underwent the highest average retreat rates 3 m/yr (table 1). Even though less than one percent of the sites in the undeveloped area of South Padre Island were advancing, the highest rate of shoreline advance (4.4 m/yr) was measured adjacent to the jetty at Mansfield Channel.

Decadal Change, 2000-2013

Rates of decade-scale Gulf shoreline change for South Padre Island and Brazos Island, calculated from lidar-derived shoreline positions between 2000 and 2013 (fig. 20), averaged 1.1 and 1.3 m/yr of retreat for net rate and linear regression rate calculations respectively.

Rates were calculated at 1,340 sites spaced at 50 m between Mansfield Channel and the Rio Grande. Net retreat occurred at 1,018 sites (76 percent) and advance occurred at 322 sites (24 percent) over the period of record (fig. 20). The overall rate is 1 m/yr less than the long-term rate of change calculated by this report (table 1).

Table 1. Comparison of historical (1937–2013) and decadal (2000–2013) shoreline change rates for South Padre and Brazos Islands.

	Historical Rates 1937–2013			Decadal Rates 2000–2013		
Study Area	No.	Net rate (m/yr)	Linear regression rate (m/yr)	No.	Net rate (m/yr)	Linear regression rate (m/yr)
Whole Study Area	1343	-2.2	-2.2	1340	-1.1	-1.3
South Padre Island (56 km)	1122	-2.4	-2.5	1120	-1.3	-1.4
Undeveloped (36 km)	720	-3.0	-3.1	719	-1.7	-2.0
Undeveloped with road (10 km)	208	-2.8	-3.0	207	-1.6	-1.7
Developed, no sea wall (2 km)	33	-1.4	-1.4	33	1.1	0.9
Developed with sea wall (8 km)	161	0.6	0.7	161	0.7	0.8
Brazos Island (11 km)	221	-1.2	-1.1	220	-0.3	-0.5

Net change rates at individual sites ranged from advance at 2.7 m/yr to retreat at 6.1 m/yr. Net advancing shorelines include a 1.4-km segment adjacent to the north jetty at Brazos Santiago Pass, a 5-km segment adjacent to the south jetty at Brazos Santiago Pass, and a 6.5-km segment within the developed area (with seawall) on South Padre Island. Net retreating shorelines include a 6-km segment north of the Rio Grande and most of the undeveloped shoreline on South Padre Island (fig. 20).

Brazos Island, between Brazos Santiago Pass and the Rio Grande, had an average net shoreline change rate of 0.3 m/yr of retreat (table 1). Retreat is occurring at 56 percent of sites on Brazos Island. The developed area, including the sea wall, experienced the lowest average net shoreline change rates within the entire study area. The shoreline in these segments advanced at an average rate of 1.1 (no seawall) and 0.7 m/yr (with seawall). The shoreline advanced at

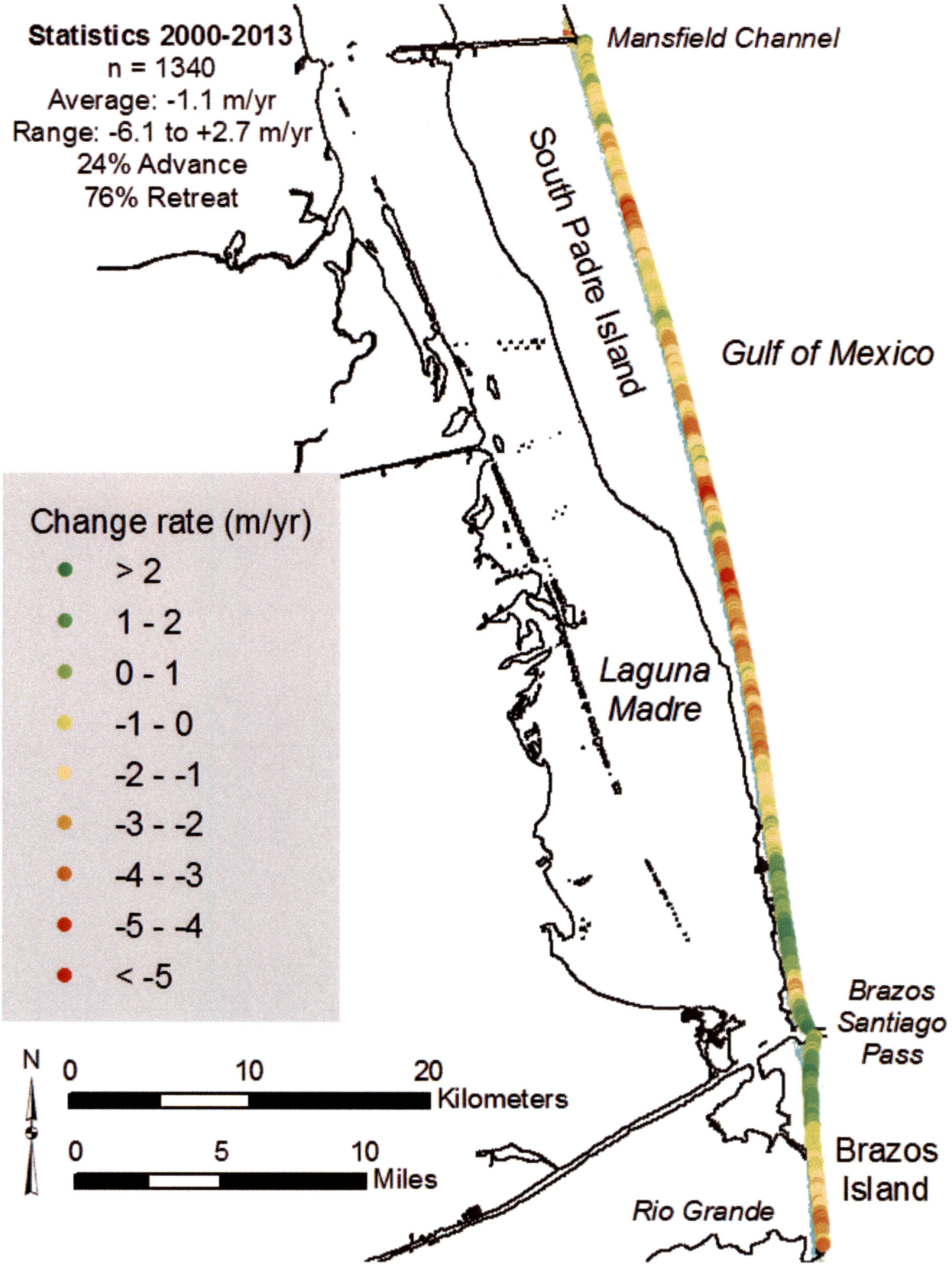

Figure 20. Net rates of decade-scale change for South Padre Island and Brazos Island calculated from shoreline positions from 2000 through 2013.

82 percent of the sites in the City of South Padre Island. The undeveloped area of South Padre Island (with and without State Park Road 100) underwent the highest average retreat rates of 1.7 m/yr (table 1). Ninety-three percent of the undeveloped sites were retreating during this time period. The highest rates of shoreline retreat (up to 6 m/yr) are found in the undeveloped section of South Padre Island near the mid-point between Mansfield Channel and Brazos Santiago Pass (fig.20).

Short-Term Change, 2010–2013

Short-term shoreline change was determined from annual airborne lidar surveys in April 2010, April 2011, February 2012, and February 2013. Rates of change can be misleading over a short period of time (3 years); therefore, change is presented as a distance rather than a rate. The South Padre Island and Brazos Island shoreline predominantly advanced between the annual airborne lidar surveys (fig. 21). Change measured along the coast was positive (advancing) at 64 percent of the 1,342 measurement sites between Mansfield Channel and the Rio Grande; the average distance that the shoreline advanced was 4.9 m (fig. 21, table 2).

Varying amounts of shoreline change were measured along the study area (figs. 21 and 22; table 2). The greatest amounts of shoreline advance, more than 30 m of net advance, were found adjacent to the south jetties at both Mansfield Channel and Brazos Santiago Pass. Shoreline retreat of more than 10 meters of landward migration of the shoreline occurred at 9 percent of the monitoring locations scattered throughout the study area. The new development area without a seawall had the greatest average net shoreline advance with 15.5 m (range -2 to 30 m). The segment with the lowest net shoreline advance was the developed area of South Padre Island with the seawall (table 2).

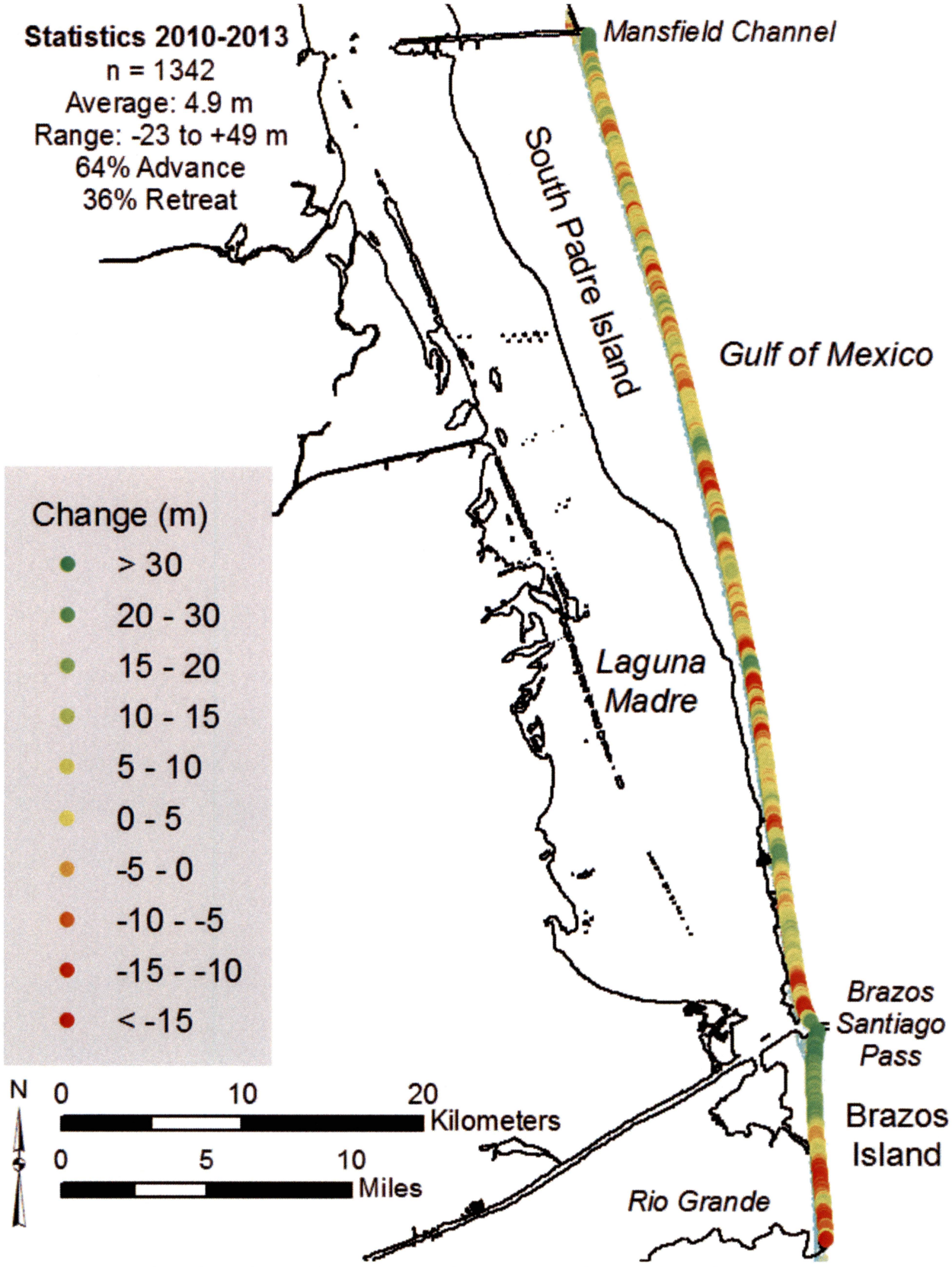

Figure 21. Net shoreline change between April 2010 and February 2013 for South Padre Island and Brazos Island.

Table 2. Net shoreline change determined from shoreline position extracted from airborne lidar data acquired in April 2010 and February 2013.

Area	No.	Net change (m)	Std. Dev. (m)	Range (m)
Whole Study Area	1342	4.9	12.0	-23 to 49
South Padre Island	1122	4.0	10.7	-23 to 49
Undeveloped	720	4.6	10.8	-20 to 49
Undeveloped w/ road	208	1.7	9.9	-19 to 29
Developed, no sea wall	33	15.5	9.6	-2 to 30
Developed	161	1.5	9.3	-23 to 20
Brazos Island	220	9.8	16.4	-19 to 43

Figure 22 graphically represents the net shoreline movement between 2010 and 2013 at each of the monitoring sites spaced 50 meters alongshore from the Rio Grande to Mansfield Channel. The green points are monitoring sites where the shoreline advanced and the red represent the sites where the shoreline retreated during the time period. Due to the scattering of the points, it is difficult to interpret a pattern or trend in the retreat or advancement of the shoreline. A running average fit line was added to the data points to assist in interpreting the shoreline movement. Running average fits are generated by taking the average of the data within a specified range on either side of a given point. A window width of 11 points was used to generate the data, including 5 points (250 m) on either side of a given data point. The average is then plotted as part of the fit line that connects all the average points. The running average plot in figure 20 illustrates the fluctuations in shoreline retreat and advance throughout the study area during this short timeframe.

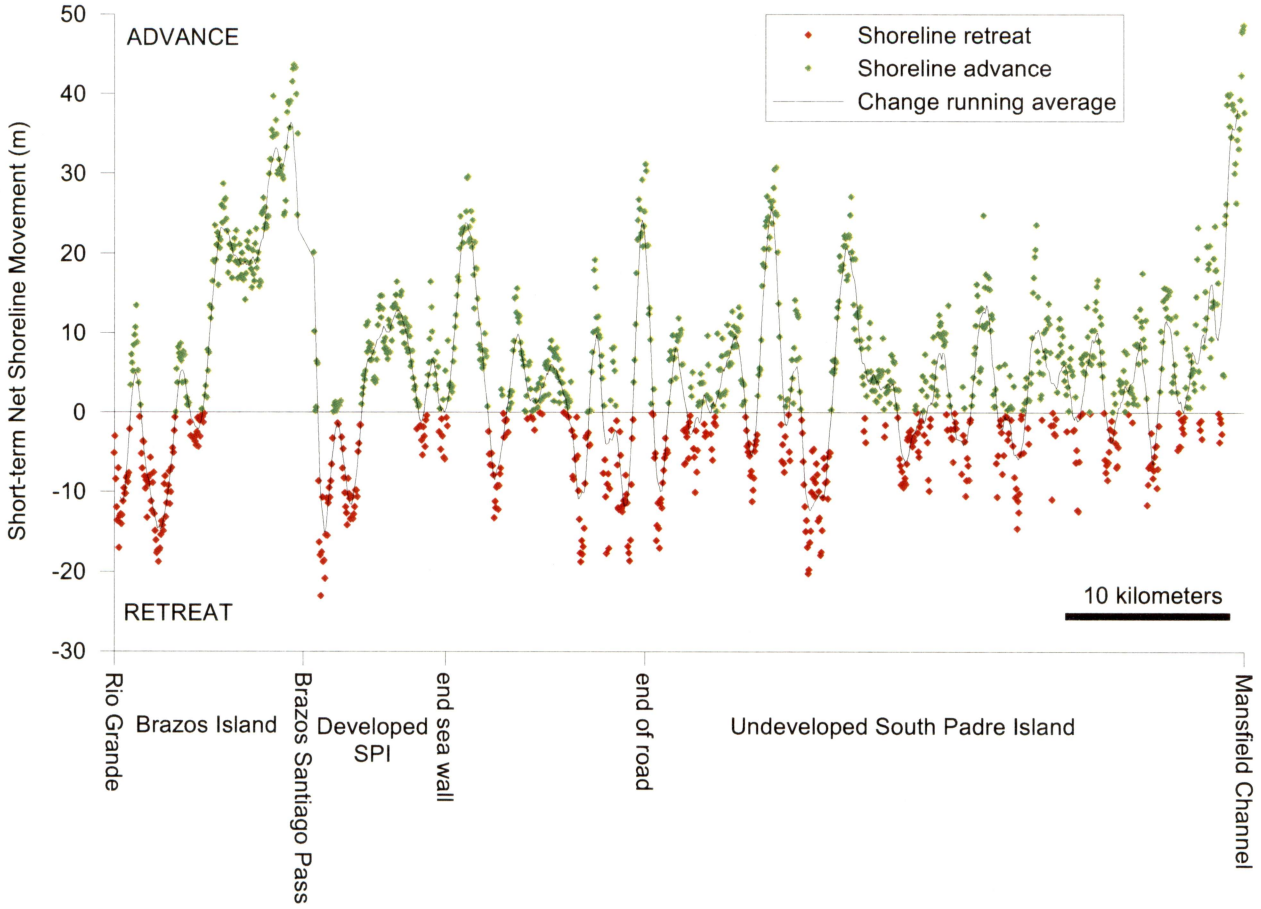

Figure 22. Short-term shoreline change between Rio Grande and Mansfield Channel showing fluctuations between advance and retreat. Points spaced every 50 meters alongshore with green representing advance and red retreat. Solid black line is running average encompassing 11 data points or 500 meters of shoreline. Running average illuminates fluctuations between advancing and retreating shorelines.

Comparison of Historical, Decadal, and Short-Term Periods

Between 1997 and 2012, the U.S. Army Corps of Engineers (USACE) completed 13 sediment bypass/beach nourishment projects using sediment dredged from Brazos Santiago Pass (Perry, 2013). Sediment was either placed directly onto select beaches in the City of South Padre Island (nourishment) or in a nearshore berm. Three of the projects (in 1997, 1999, and 2002) placed sand both as nourishment and in the nearshore berm. The projects in 2000, 2005, 2009, 2010, 2011, and 2012 were beach nourishment projects. The projects in 2003, 2006, 2007, and 2008 placed sediment into the nearshore berms.

These sediment bypass/beach nourishment projects are likely one factor responsible for the difference between the lower (less negative) decadal shoreline change rate of -1.1 m/yr and the historical rate of -2.2 m/yr. Sediment bypass/beach nourishment may also be responsible for the average shoreline advancement documented between 2010 and 2013 (fig. 23). Figure 22 compares the historical shoreline change rates at the monitoring sites in the study area with the decade-scale (2000–2013) change rates and the short-term (2010–2013) shoreline movement. The trend of the decade-scale change rates mimics the long-term trends along the length of the study area, except that the decade-scale rates are generally higher on the graph (lower retreat, higher advancement rates). A notable exception is adjacent to the south jetty at Mansfield Channel, where the highest rates of shoreline advancement are recorded in the historical record, whereas between 2000 and 2013 the shoreline was retreating (~1 m/yr) or stable. Fluctuations also exist in the decade-scale shoreline change rates alongshore that are generally smoothed throughout the historical rates. This trend mimics the fluctuations between advancement and retreat noted in the short-term shoreline change. The movement of the shoreline in the short-term and decade-scale monitoring periods could represent the redistribution of sediments from the sediment bypassing/beach nourishment projects that have taken place since 1997.

The advance and retreat of shorelines following nourishment projects on South Padre Island has also been documented by students participating in the Texas High School Coastal Monitoring Program at all three of their sites. Figure 24 is the SPI02 THSCMP monitoring site located at Beach Access 13 (Moonlight Circle), approximately 4.5 km north of Brazos Santiago Pass, or the mid-point of the developed area within the seawall on South Padre Island (fig. 1). The Port Isabel High School students have been measuring fluctuations in the movement of the shoreline (green line, fig. 24) with an overall trend of shoreline advancement as a result of beach nourishment projects at this study site. Sediment volume (red line) in the beach profile has also increased through time at this study site.

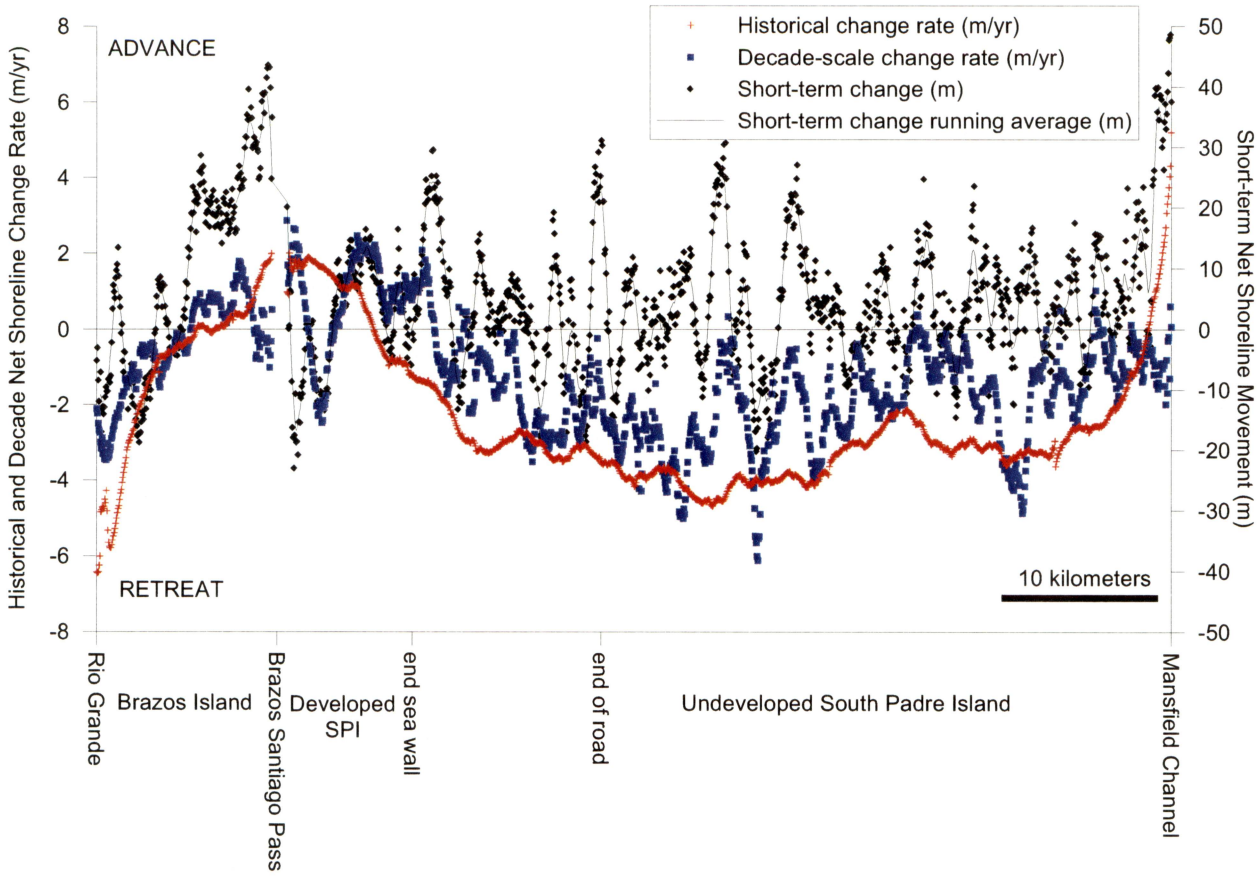

Figure 23. Comparison of historical and decade-scale net shoreline change rates (m/yr) with short-term net shoreline movement (m).

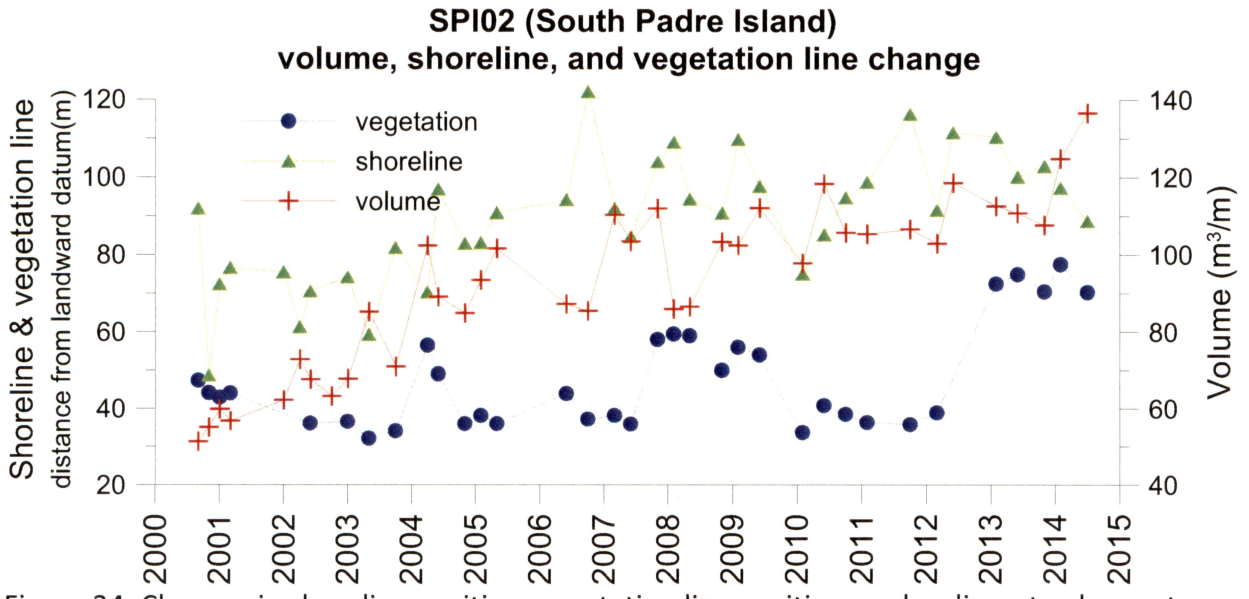

Figure 24. Changes in shoreline position, vegetation line position, and sediment volume at SPI02 on South Padre Island as measured by Port Isabel High School students participating in Texas High School Coastal Monitoring Program.

VOLUMETRIC ANALYSIS

The DEM created by this study provides a wealth of information about the beach and dune system of South Padre and Brazos Islands. We sliced the DEM at multiple elevation thresholds to examine the volume of sediment in the beach and dune system. We wrote a program to calculate the total volume of sand stored above the 1-meter elevation threshold in the beach and dune system. The beach and dune system was defined as the area falling landward of the extracted shoreline and seaward of the mapped back-dune line. Volumes were also calculated above the 2-meter elevation threshold through 6-meter elevation thresholds. Examining the volume of sediment stored above threshold elevations in the beach and dune system can be helpful for understanding several important characteristics related to coastal geomorphology. These include (1) susceptibility to storm surge and flooding at differing surge heights, (2) sand storage within the beach and dune system, (3) maturity and extent of the dunes, and (4) resistance and recoverability from chronic and instantaneous erosion events. Extracting volume information from previous lidar surveys also provides a means to monitor volume change over time.

We calculated volume statistics for the beach and dune system within the study area from three lidar surveys: those from 2000, 2010, and 2013 (fig. 25, table 3). Plots of threshold elevation against average volume exceeding that elevation for each time period reveal a rapid reduction in volume of sediment as threshold elevations are increased. For example, at the 3-m elevation, the dune contains 63.1 m^3/m (2000) to 87 m^3/m (2013) of sand at or above that elevation. Above the 4-m threshold, a little more than half that volume of sand (32.4 m^3/m in 2000 to 45.5 m^3/m in 2013), is at or above that elevation. The reduction of volume by approximately half with each 1-m increase in threshold elevation is constant throughout the 1- to 6-m elevation ranges. Both figure 25 and table 3 show that beach and dune system volume in the study area has steadily increased at each threshold elevation since 2000.

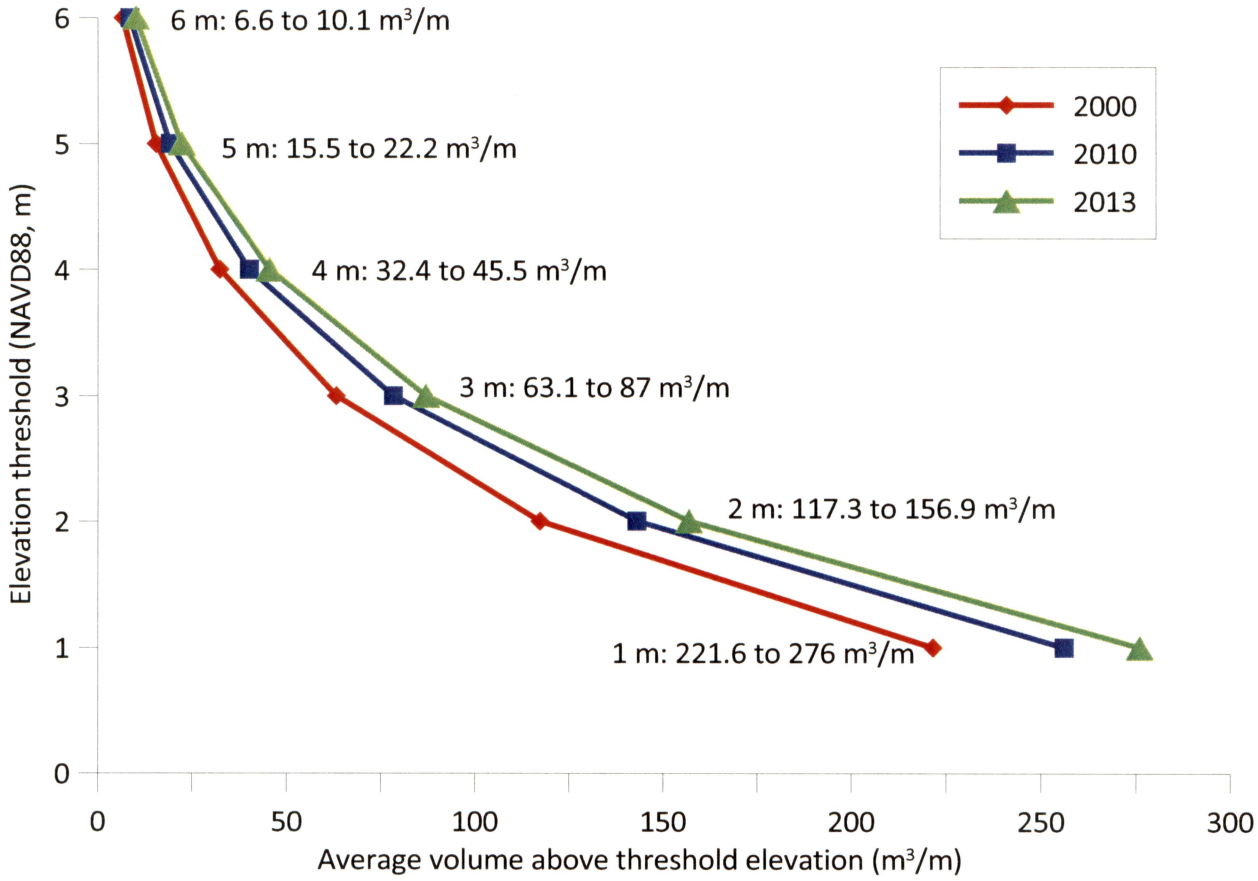

Figure 25. Average volume (m^{3}/m) of sand per meter of shoreline above threshold elevations in 2000, 2010, and 2013 for Brazos and South Padre Islands. Threshold volume increases through time.

Table 3. Total combined volume of sand above threshold elevations in beach and dune system on Brazos and South Padre Islands.

Threshold Elevation (m)	Total Volume (m3)		
	2000	2010	2013
6	444,477	571,654	676,397
5	1,039,879	1,293,325	1,495,931
4	2,178,777	2,700,680	3,060,326
3	4,249,298	5,270,829	5,853,264
2	7,893,530	9,629,415	10,559,058
1	14,910,923	17,232,382	18,572,063

Plots of volume above different threshold elevations were constructed for each island (Brazos and South Padre, fig. 26a) as well as for the different South Padre Island segments examined in the shoreline change analysis (fig. 26b). The volume statistics represented in figure 26 were calculated from the 2013 lidar data. Information from the 2000 and 2010 lidar datasets can be found in Appendix B. Because the islands and island segments are different lengths, the volume calculations were normalized to represent the volume of sand in the beach and dune system per meter of shoreline.

Much less sand is stored in the beach and dune system on Brazos Island than on the whole of South Padre Island (fig. 26a). This is due to a generally narrower beach and dune system on Brazos Island. The trend of the volume above threshold elevations on Brazos Island is very similar to the curve from the sites within the developed portion of South Padre Island that is backed by the seawall. The width of the beach and dune system within this developed section of South Padre Island is limited owing to the seawall serving as the fixed back dune line. The developed segment of South Padre Island contains few areas with sand storage and dune crests greater than 4 m (fig. 27). A small area near the southernmost point of South Padre Island (adjacent to Isla Blanca Park) has a mature dune system with dune crests greater than 6 meters (fig. 28).

The undeveloped areas of South Padre Island have an extensive and mature foredune area, except for areas of washover features (fig. 29). Storage capacity within these sections (with and without the road) is extremely high owing to the lack of development constraining the dune system. The volume of sand at the higher elevation thresholds is slightly lower for the undeveloped area with State Park Road 100 than for the segment without the road, probably as a result of maintenance removal of sand to keep the road clear. The volume of sand within the small developed segment without a seawall contains significantly more sand, particularly at the lower threshold elevations, than the segment with the seawall. The volume trend more closely mimics what is observed in the undeveloped areas.

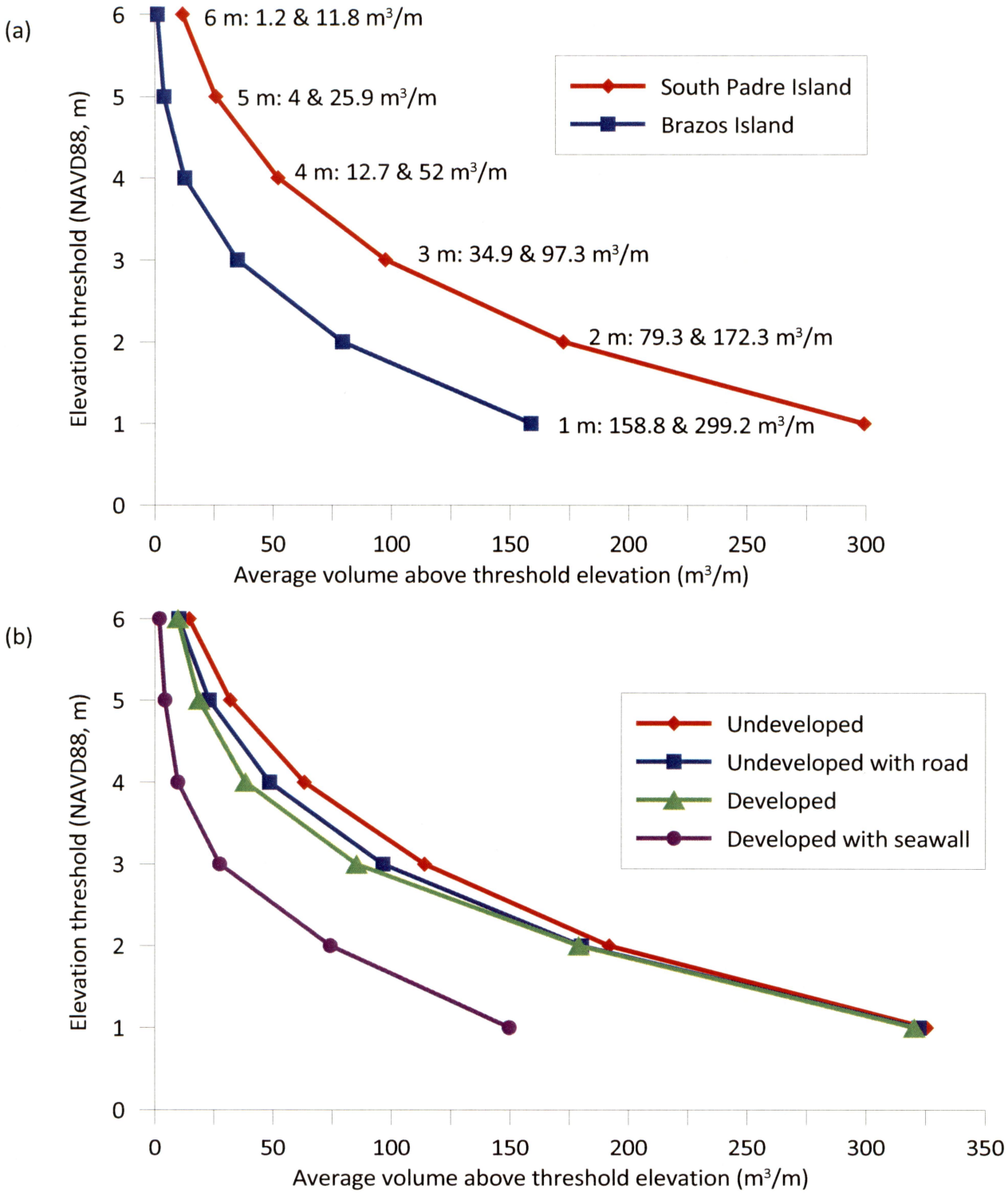

Figure 26. Average volume (m^3/m) above threshold elevations for (a) Brazos and South Padre Island and (b) South Padre Island segments calculated from 2013 lidar-derived DEMS.

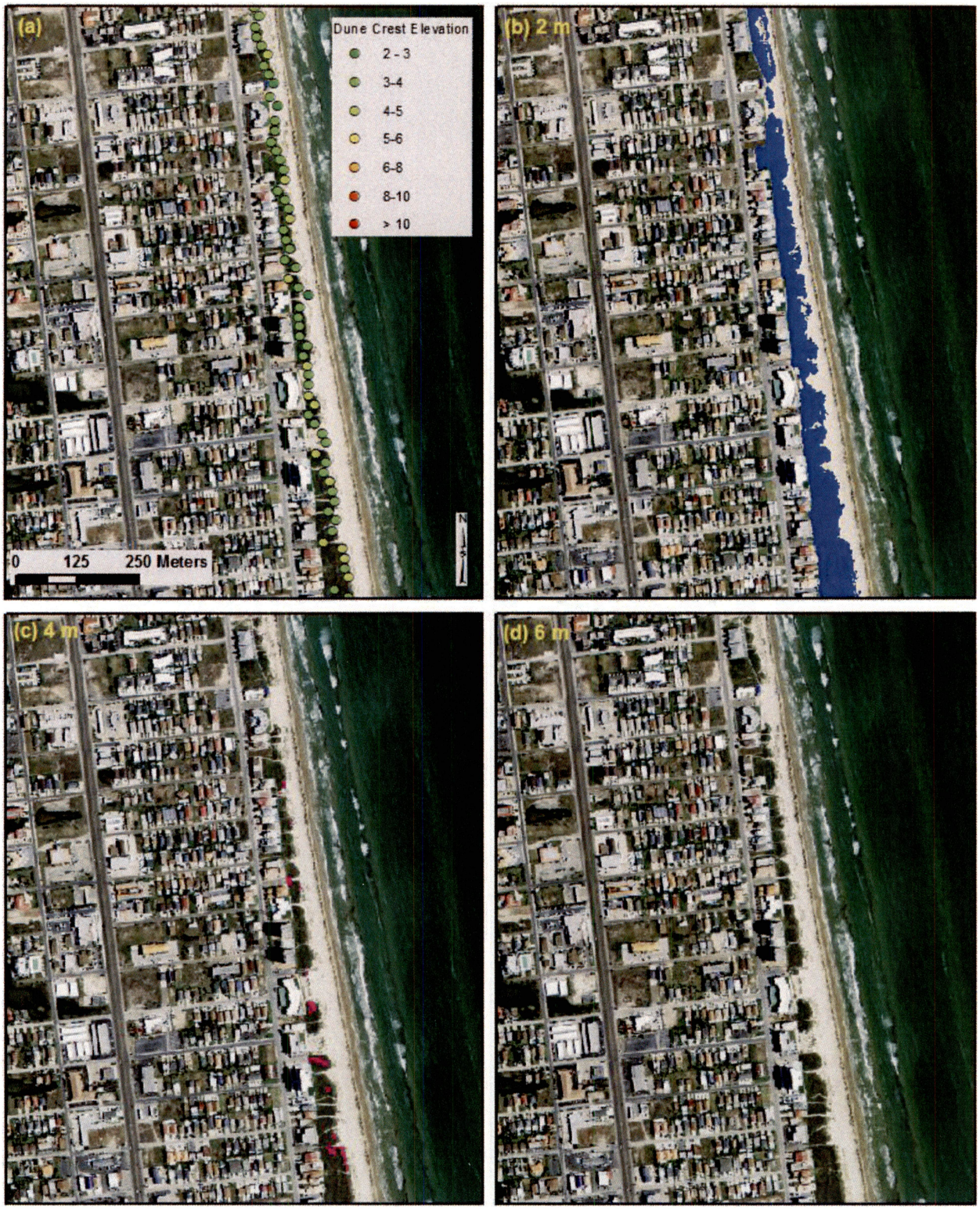

Figure 27. South Padre Island developed segment with seawall (a) showing maximum dune crest elevations. Areas of threshold elevations greater than (b) 2 m, (c) 4 m, and (d) 6m. Note there are no areas greater than 6 m in the beach and dune system.

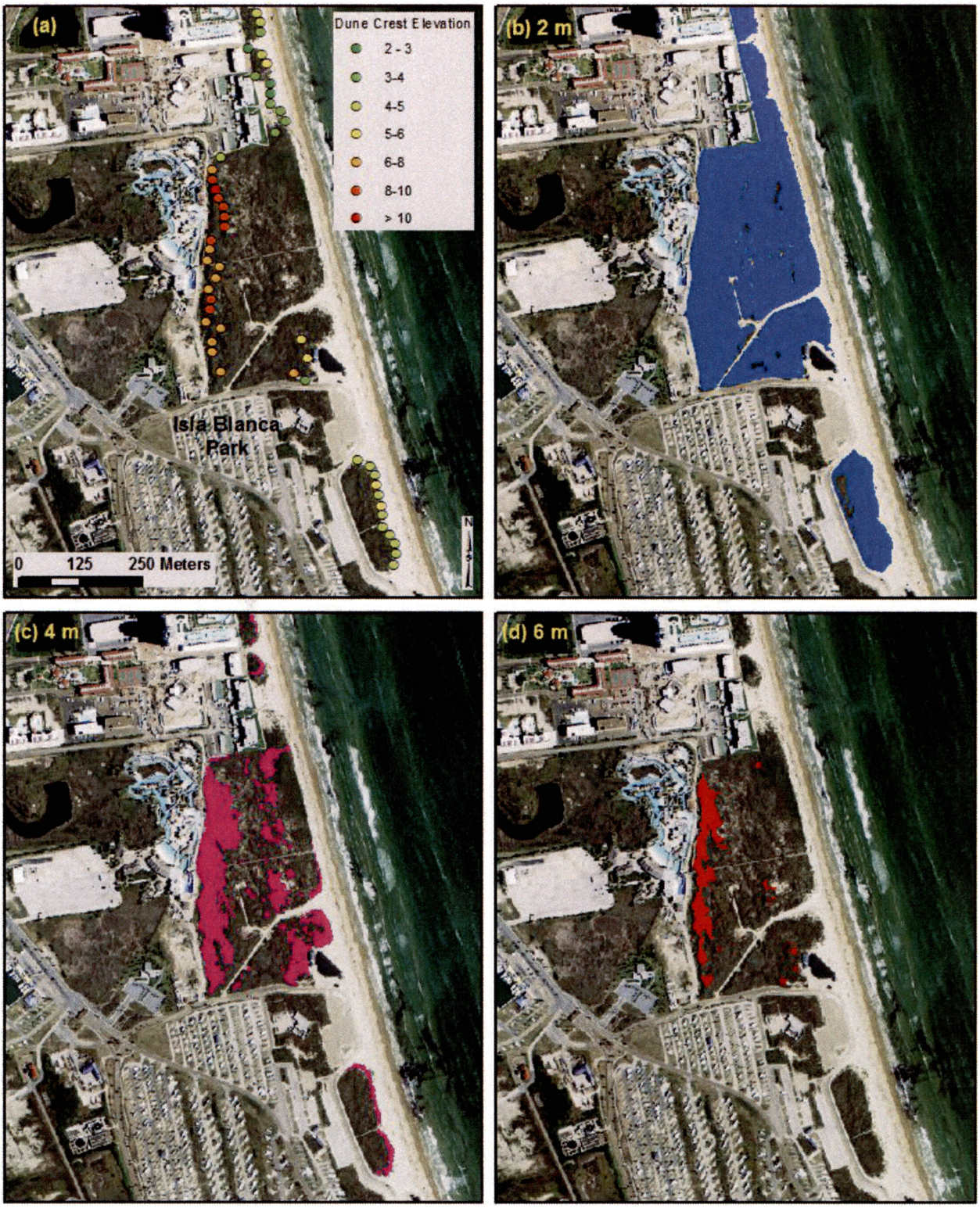

Figure 28. Developed segment of South Padre Island with seawall (a) showing maximum dune crest elevations. Areas of threshold elevations greater than (b) 2 m, (c) 4 m, and (d) 6 m. This area north of Brazos Santiago Pass and Isla Blanca Park is only section with mature foredune with dune crests greater than 6 meters.

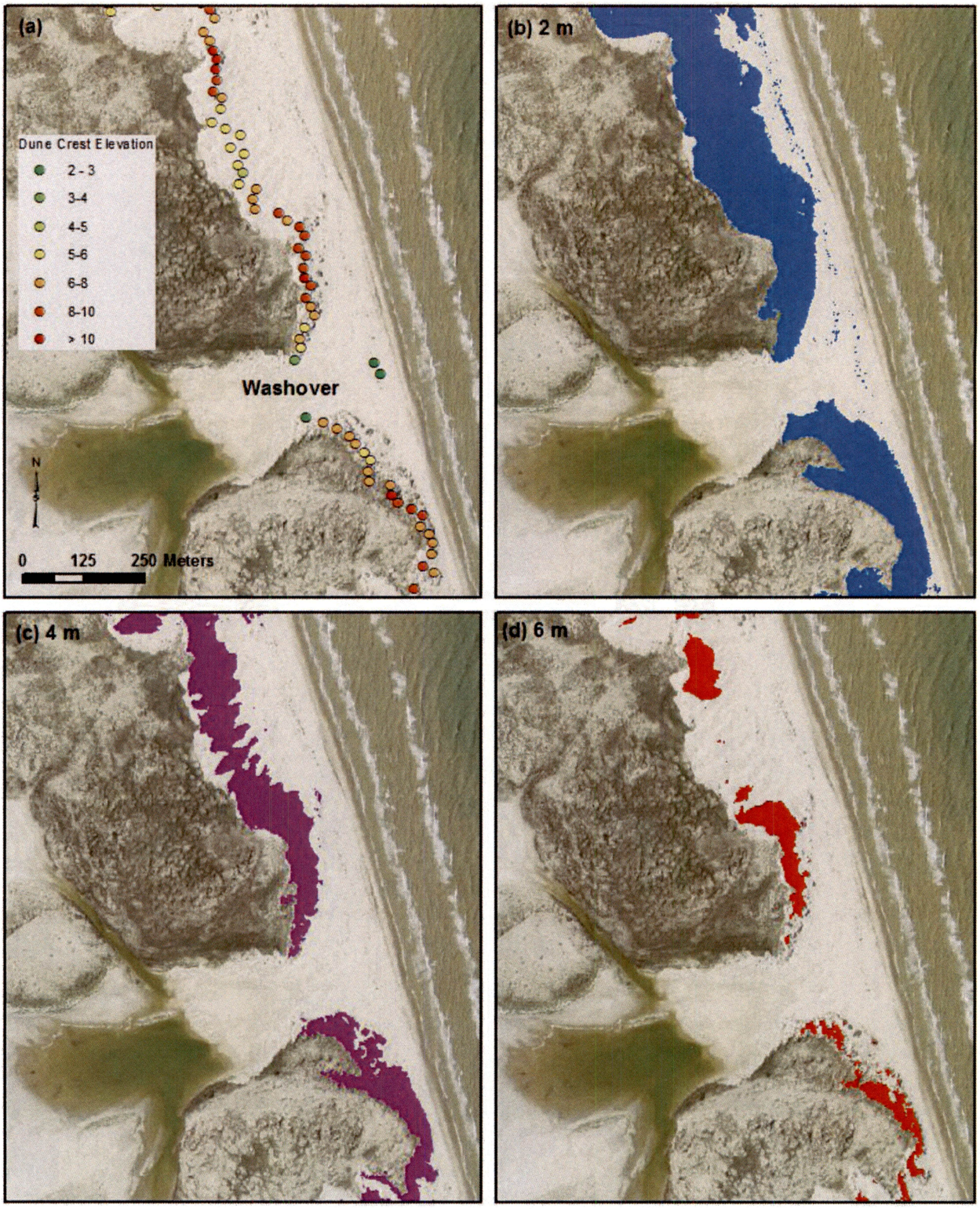

Figure 29. Undeveloped South Padre Island (a) showing maximum dune crest elevations. Areas of threshold elevations greater than (b) 2 m, (c) 4 m, and (d) 6m.

Upon examining the volume change between the 2000, 2010, and 2013 datasets, the segment of South Padre Island that is developed and has no seawall is the only segment where the volume of sand at the higher threshold elevations (> 4 m) is decreasing through time (fig. 30). The volume trends through time for Brazos Island, South Padre Island, and the South Padre Island segments can be found in Appendix C. The higher-threshold elevations for Brazos Island, the developed segment with the seawall, and the undeveloped segment with the road have kept a fairly constant volume of sand, whereas the lower-threshold elevations (1–3 m) are increasing in volume. The undeveloped segment of South Padre Island (the largest segment) has increased in volume across all of the threshold elevations.

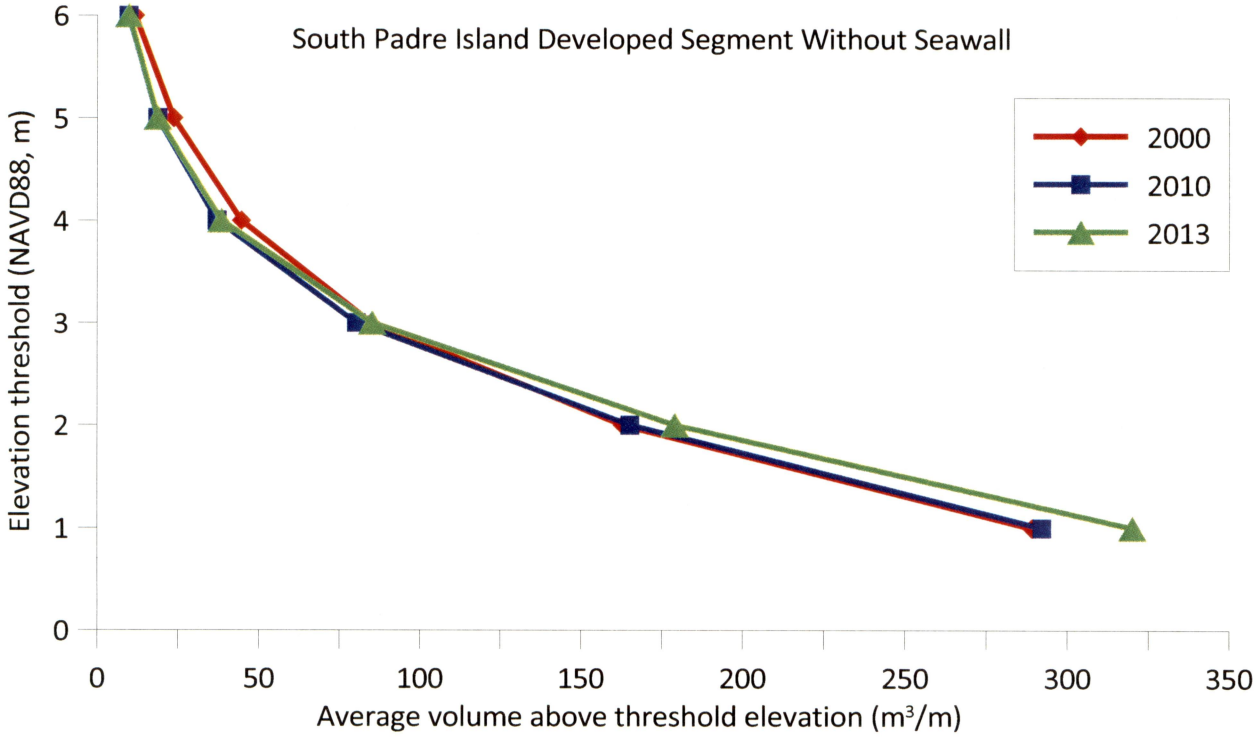

Figure 30. Average volume (m^3/m) of sand per meter of shoreline above threshold elevations in 2000, 2010, and 2013 for developed area of South Padre Island without seawall. Volume at higher threshold elevations decreases through time.

Volumetric analyses of the beach and dune system on South Padre Island and Brazos Island are important for understanding the current sand storage of the environment and which areas are more susceptible to storm surge of varying levels. We have created a website (http://www.beg.utexas.edu/coastal/dune_sp.php) where scientists, coastal developers,

decision makers, and the general public can access the data, particularly the GIS datasets, described in this report. Volume calculations are available interactively through the data viewer and by downloading the Beach/Dune Volumes GIS shapefile, which includes points every 5 meters alongshore in the study area.

BATHMETRIC LIDAR ASSESSMENT

The bathymetric data collection portion of this project was our first opportunity to examine the depth capability and water-clarity limitations of the Chiroptera on the open Gulf of Mexico coast. Bathymetric lidar is a fundamental advance in the ability to acquire nearshore data, but Chiroptera was previously untested under murky-water conditions that are typical of the Texas coast.

We compared lidar-derived bathymetry acquired in January 2013 with bathymetric data obtained from fifty-three single-beam sonar lines collected offshore of the City of South Padre Island by Naismith Marine Services, Inc., in October 2012 (fig. 31). The time elapsed between the sonar survey and our lidar survey was four months. We expected to see some differences in the nearshore bar positions, but the data are still extremely beneficial to our understanding of waveform characteristics, lidar returns, and laser-penetration depth within the study area.

The southernmost sonar transect helped to verify that actual seafloor returns were captured in the area adjacent to the north jetty at Brazos Santiago Pass (fig. 32). The protected waters in this area (with less sediment suspended in the water column at the time of the survey) were sufficiently clear to allow the bathymetric laser to penetrate the water column. Returns classified by AHAB's LSS software as "bottom" in this small part of the study area were true seafloor returns. The lidar data points (blue points in fig. 32) illustrate a smooth seafloor surface similar to the sonar data points (red). The differences between the two seafloor surfaces can be attributed to migration of the

Figure 31. Single-beam sonar lines collected October 2012. Data from Naismith Marine Services, Inc.

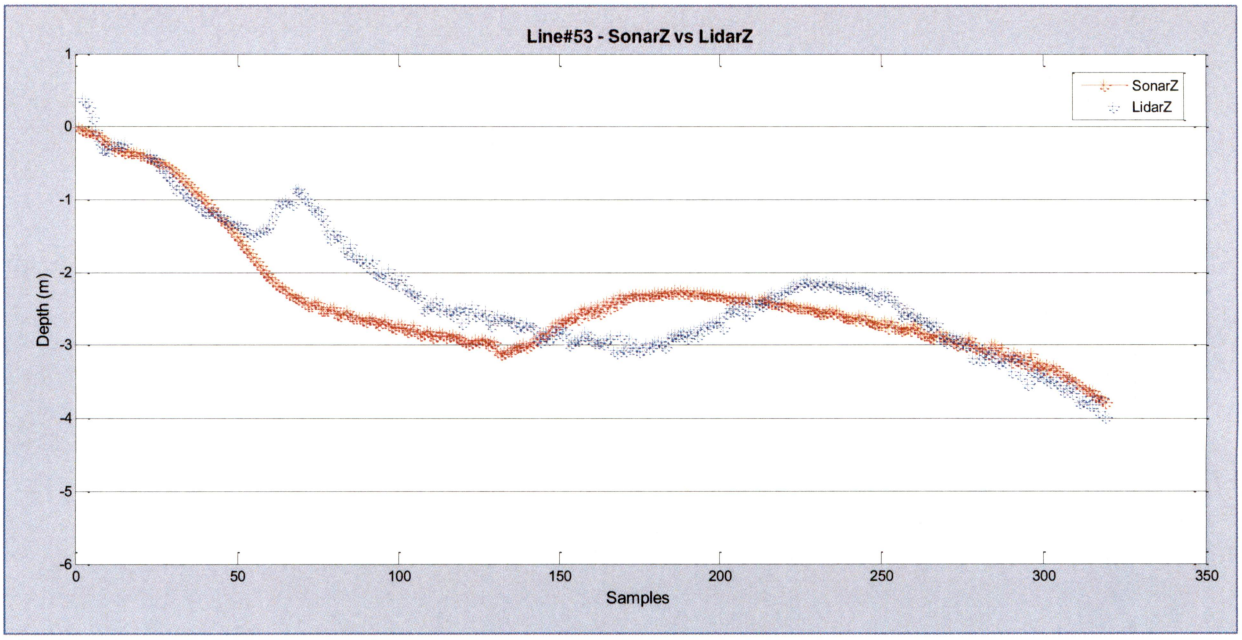

Figure 32. Comparison of lidar (blue) with single-beam sonar (red) from southernmost transect line near north jetty of Brazos Santiago Pass.

nearshore bars between the one data collection and the next. A second area of true seafloor returns occurred adjacent to the north jetty of Mansfield Channel.

Water conditions, specifically wave activity and clarity, in the majority of the study area were not ideal for the Chiroperta green laser to penetrate the water column or even the water surface. LSS classified "bottom" returns were actually reflections within the water column, not true seafloor returns. Figure 33 illustrates the noisy returns of the bathymetric laser system as compared to the sonar data. The red points of the sonar data show a smooth seafloor surface, whereas the blue points (lidar) are scattered throughout the water column. A strong subsurface return waveform should have two distinctive peaks in the waveform (fig. 34a)—the first from the water's surface and the second from the bottom surface (seafloor), where the laser is reflected back to the receiver. Noisy waveforms will have indistinct or multiple smaller return peaks (fig. 34b) as a result of scattering off of sediment suspended in the water column.

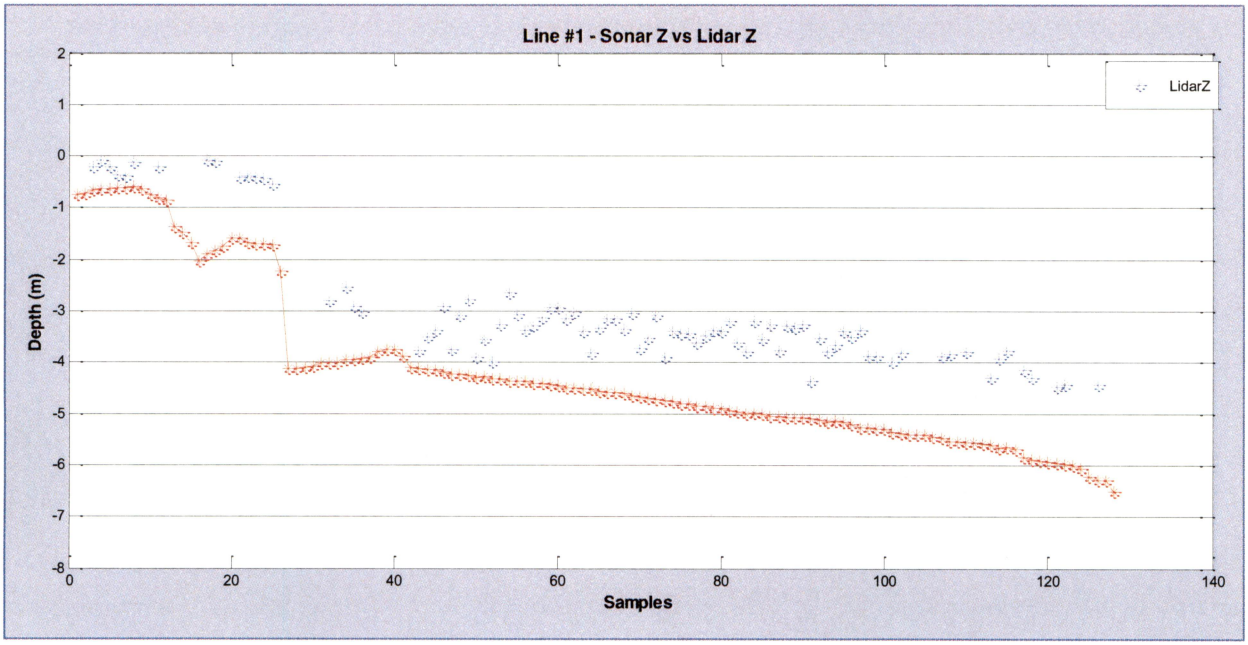

Figure 33. Comparison of lidar bottom returns (blue) with sonar data points (red) from northernmost transect. Sonar points form smooth seafloor surface; lidar returns scattered throughout the water column owing to lack of clarity.

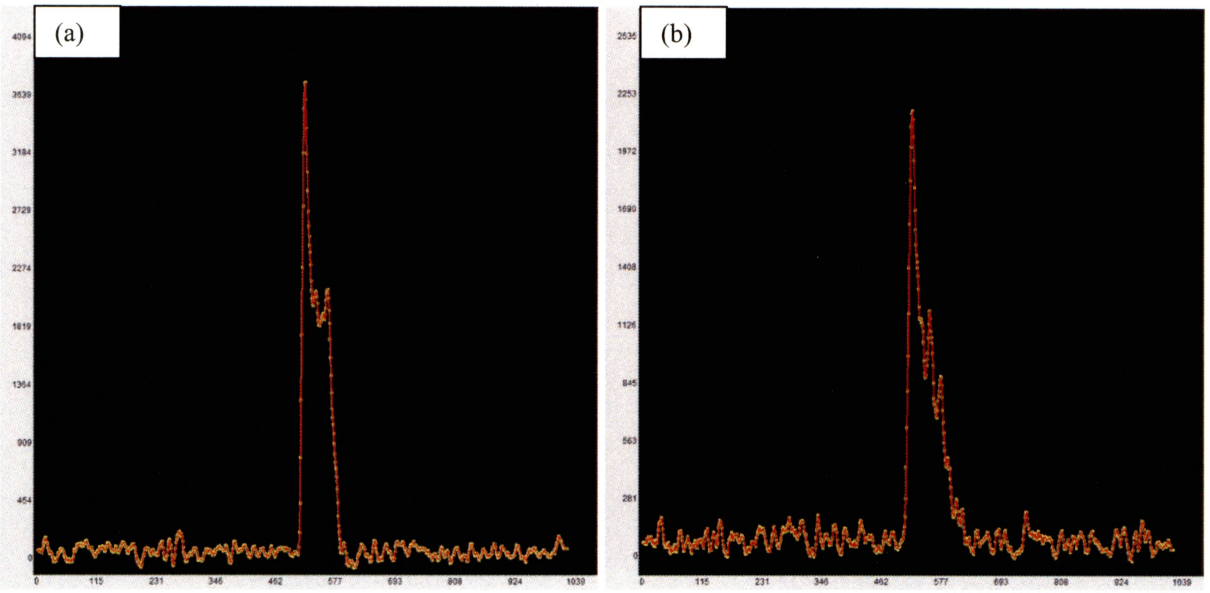

Figure 34. Comparison of waveform returns in (a) clear water with two strong peaks representing water surface and seafloor with (b) noisy waveform pattern in murky water. Distinct peak represents water surface, but multiple smaller peaks follow, representing scattering of laser pulse owing to sediment in water column.

We believe that with additional analysis of the bathymetric waveforms, additional seafloor returns may be extracted from the data in this and other coastal areas with less than ideal water conditions. This is a critical area of active research at BEG and AHAB. A "murky water" algorithm is under development at AHAB that is expected to improve characterization of true seafloor returns and minimize misclassification of water-column returns.

CONCLUSIONS

A topographic and bathymetric lidar and aerial imagery survey of South Padre Island and Brazos Island, Texas, was conducted in February 2013. A high-resolution DEM was constructed from the data, allowing extraction of critical coastal features including shoreline, potential vegetation line, landward dune boundary, geomorphic units, maximum dune crest elevation and position, and beach and dune volume.

By combining CIR aerial imagery and topographic lidar data, we mapped geomorphic units along South Padre and Brazos Islands. Wetland habitats were interpreted from the 2013 CIR aerial imagery, in accordance with the National Wetlands Inventory (NWI) classification scheme. Draping CIR imagery on the lidar DEM was beneficial for mapping upland geomorphic units, which included washover channel and fan, fore-island dune complex, fore-island dune ridge, vegetated barrier flat, mid-island dune complex, and back-island dune complex.

Shoreline change was determined on historical, decadal, and short-term scales. Historical rates of long-term shoreline change for South Padre Island and Brazos Island were calculated from shorelines from 1937 to 2013. The shoreline in the study area has retreated at 86 percent of the monitoring sites, with an average rate of 2.2 m/yr. Over the period 2000 to 2013, the rates decreased to 1.1 m/yr of retreat (76 percent of sites retreating). Between 2010 and 2013, 64 percent of monitoring sites advanced an average distance of 4.9 m.

The 2013 DEMs were used to examine beach and dune volumes above threshold elevations ranging from 1 to 6 m. The plots created from the evaluation of the volumes are useful in assessing sand storage, susceptibility to storm-surge flooding, and erosion susceptibility and recovery potential. The total volume of sand in the beach and dune system varied among the different coastal segments (with a lower volume in the developed segments of South Padre Island and a higher volume in the undeveloped segments). A common trend among the different segments is that volume is incrementally reduced by approximately half with each 1-m increase in threshold elevation.

The bathymetric data collection portion of this project was our first opportunity to examine the depth capability and water-clarity limitations of the Chiroptera on the open Gulf of Mexico coast. Definitive seafloor returns were identified in two areas adjacent to the north jetty at Mansfield Channel and the north jetty at Brazos Santiago Pass. In other areas, where water is less clear, Chiroptera software misclassified many water-column returns as seafloor returns. Additional analysis of the bathymetric waveforms will be necessary to establish whether true seafloor returns can be extracted from the 2013 survey. This analysis is the subject of active research being conducted jointly by Bureau researchers and AHAB technicians.

ACKNOWLEDGMENTS

This project was supported by grant no. 13-030-000-6895 from the Texas General Land Office to the Bureau of Economic Geology, The University of Texas at Austin. Tiffany L. Caudle and Thomas A. Tremblay served as the co-principal investigators. This project was funded under a Coastal Management Program (Cycle 17) grant made available to the State of Texas by the U.S. Department of Commerce, National Oceanic and Atmospheric Administration, pursuant to the Federal Coastal Zone Management Act of 1972, NOAA Award No. NA12NOS4190021. Additional funds were provided by the State of Texas Advanced Oil and Gas Resource Recovery (STARR). Sean Hilbe (General Land Office) served as project manager. In addition to Caudle and Tremblay, the following Bureau staff contributed to the project: John Andrews, Aaron Averett,

Sojan Mathew, Jeffrey Paine, and Kutalmis Saylam. Aircraft support for the lidar survey was provided by the Texas Department of Transportation. The views expressed herein are those of the authors and do not necessarily reflect the views of the project sponsors.

REFERENCES

Brown, L. F., Jr., Brewton, J. L., Evans, T. J., McGowen, J. H., White, W. A., Groat, C. G., and Fisher, W. L., 1980, Environmental geologic atlas of the Texas Coastal Zone, Brownsville–Harlingen area: The University of Texas at Austin, Bureau of Economic Geology, Special Publication, 140 p.

Cowardin, L. M., Carter, V., Golet, F. C., and LaRoe, E. T., 1979, Classification of wetlands and deepwater habitats of the United States. U. S. Department of the Interior, Fish and Wildlife Service, Washington, D.C. FWS/OBS-79/31.

Gibeaut, J. C., Gutierrez, Roberto, and Hepner, Tiffany, 2002, Threshold conditions for episodic beach erosion along the southeast Texas coast: Gulf Coast Association of Geological Societies Transactions, v. 52, p. 323-335.

Gibeaut, J. C., and Caudle, Tiffany, 2009, Defining and mapping foredunes, the line of vegetation, and shorelines along the Texas Gulf Coast: Texas A&M University Corpus Christi, Harte Research Institute and The University of Texas at Austin, Bureau of Economic Geology, final report prepared for the Texas General Land Office contract no. 07-005-22 and National Oceanic and Atmospheric Administration award no. NA06NOS4190219, 14 p.

Morton, R. A., 1977, Historical shoreline changes and their causes, Texas Gulf Coast: Gulf Coast Association of Geological Societies Transactions, v. 27, p. 352–364. Reprinted as Bureau of Economic Geology Geological Circular 77-6, 13 p.

Morton, R. A., Miller, T. L., and Moore, L. J., 2004, National assessment of shoreline change, part 1: historical shoreline changes and associated coastal land loss along the U.S. Gulf of Mexico: U.S. Geological Survey Open-File Report 2004-1043, 42 p.

Morton, R. A., Miller, T., and Moore, L. J., 2005, Historical shoreline changes along the US Gulf of Mexico: a summary of recent shoreline comparisons and analyses: Journal of Coastal Research, v. 21, p. 704-709.

Morton, R. A., and Paine, J. G., 1990, Coastal land loss in Texas: an overview: Transactions, Gulf Coast Association of Geological Societies, v. 40, p. 625-634.

Morton, R. A., and Pieper, M. J., 1975, Shoreline changes on Brazos Island and South Padre Island (Mansfield Channel to mouth of the Rio Grande), an analysis of historical changes of the Texas Gulf shoreline: The University of Texas at Austin, Bureau of Economic Geology, Geological Circular 75-2, 39 p.

Paine, J. G., Mathew, S., Caudle, T., 2011. Texas Gulf shoreline change rates through 2007: University of Texas at Austin, Bureau of Economic Geology, report prepared under General

Land Office contract no. 10-041-000-3737 and National Oceanic and Atmospheric Administration award no. NA09NOS4190165, 38 p. + CD-ROM.

Paine, J. G., Mathew, Sojan, and Caudle, Tiffany, 2012, Historical shoreline change through 2007, Texas Gulf coast: rates, contributing causes, and Holocene context: GCAGS Journal, v. 1, p. 13-26.

Paine, J. G., and Morton, R. A., 1989, Shoreline and vegetation-line movement, Texas Gulf Coast, 1974 to 1982: The University of Texas at Austin, Bureau of Economic Geology Geological Circular 89-1, 50 p.

Perry, M. C., 2013, Monitoring survey of South Padre Island 2013 annual beach report: HDR Engineering, Inc., report for the Texas General Land Office, 10 p+ survey drawings.

Thieler, E. R., Himmelstoss, E. A., Zichichi, J. L., and Ergul, Ayhan, 2009, Digital Shoreline Analysis System (DSAS) version 4.0 — an ArcGIS extension for calculating shoreline change: U.S. Geological Survey Open-File Report 2008-1278. [current version 4.2]

White, W. A., Morton, R. A, Kerr, R. S., Kuenzi, W. D., and Brogden, W. B., 1978, Land and water resources, historical changes, and dune criticality: The University of Texas at Austin, Bureau of Economic Geology, Report of Investigations No. 92., 46 p.

White, W. A., Tremblay, T. A., Waldinger, R. L., Hepner, T. L., and Calnan, T. R., 2005, Status and trends of wetland and aquatic habitats on barrier islands, Freeport to East Matagorda Bay, and South Padre Island: The University of Texas at Austin, Bureau of Economic Geology, final report prepared for the Texas General Land Office and National Oceanic and Atmospheric Administration, under GLO contract nos. 04-044 and 04-045, a report of the Coastal Coordination Council pursuant to National Oceanic and Atmospheric Administration Award No. NA03NOS4190102, 100 p.

APPENDIX A: IMAGEMAGICK SCRIPT

Below is a sample ImageMagick script for one image (of 1886 total images):

```
# --- for image "1000.tif" exported from Phocus  ----------
# re-order channels:
convert  1000.tif      \
-set colorspace  RGB    \
-separate             \
-swap 0,2             \
-swap 1,2             \
-combine              \
-channel RGB          \
/cygdrive/z/2012.08_alaska/john_temp/01_swap/1000_swap.tif # writes intermediate file "1000_swap.tif"

# 'isolate' IR to 1st (aka red or 'r') channel by subtracting it from chan2 (g) and chan3 (b):
convert /cygdrive/z/2012.08_alaska/john_temp/01_swap/1000_swap.tif    \
-set colorspace  RGB               \
-channel  G  -fx '(g*1.0) - (r*.6)'  \
-channel  B  -fx '(b*1.0) - (r*.6)'  \
-channel RGB                       \
/cygdrive/z/2012.08_alaska/john_temp/02_irsubtr/1000_irsubtr.tif

# ------------------------------------------------------------
```

Average volume (m^3/m) above threshold elevations for (a) Brazos and South Padre Island and (b) South Padre Island segments calculated from the 2000 lidar-derived DEMS.

(a)

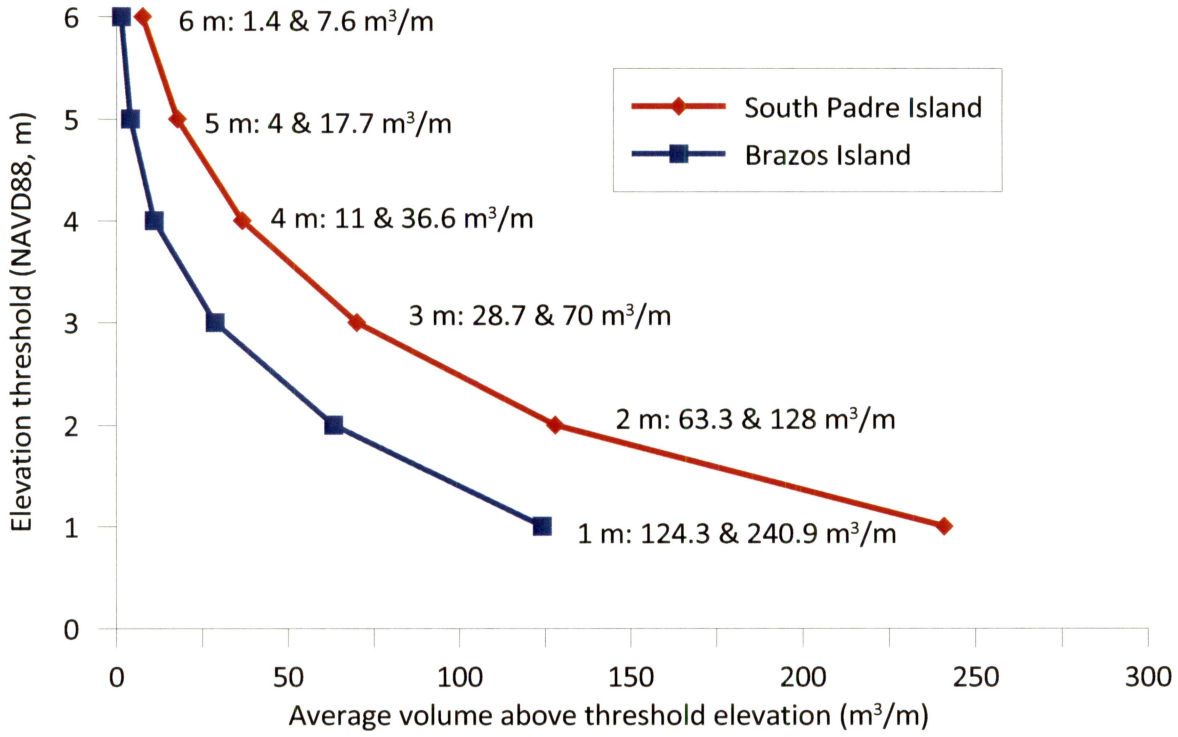

(b)

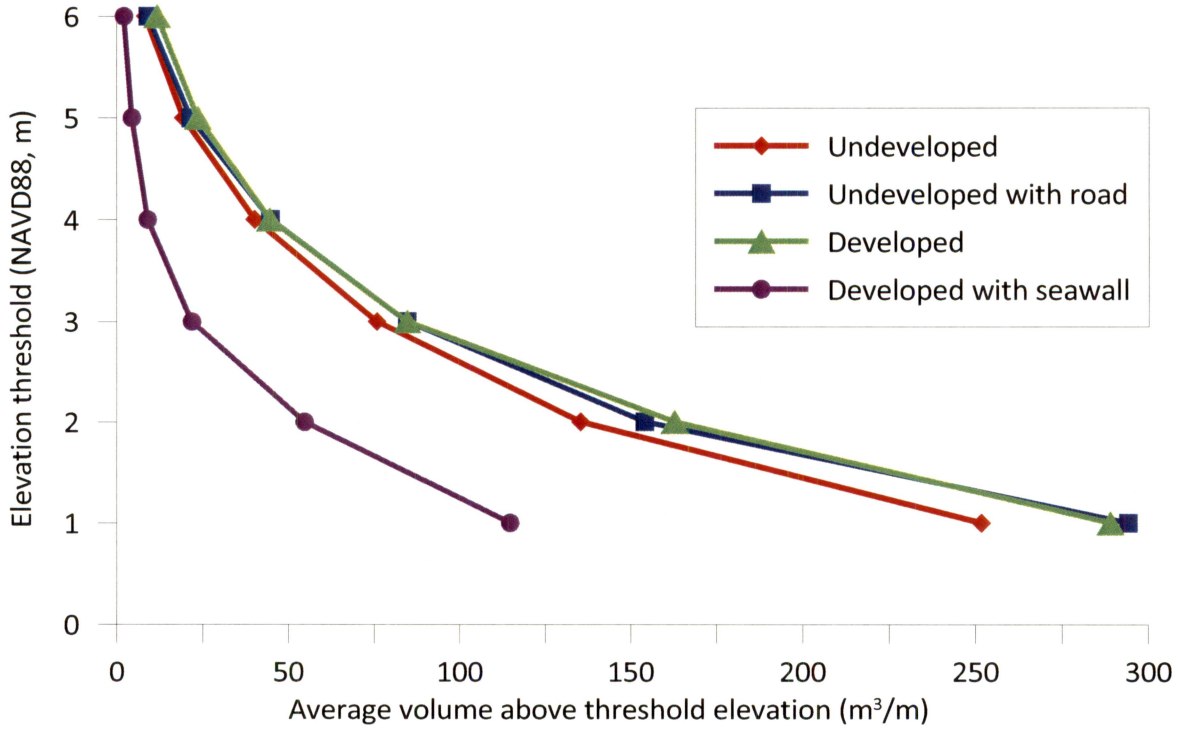

Average volume (m^3/m) above threshold elevations for (a) Brazos and South Padre Island and (b) South Padre Island segments calculated from the 2010 lidar-derived DEMS.

(a)

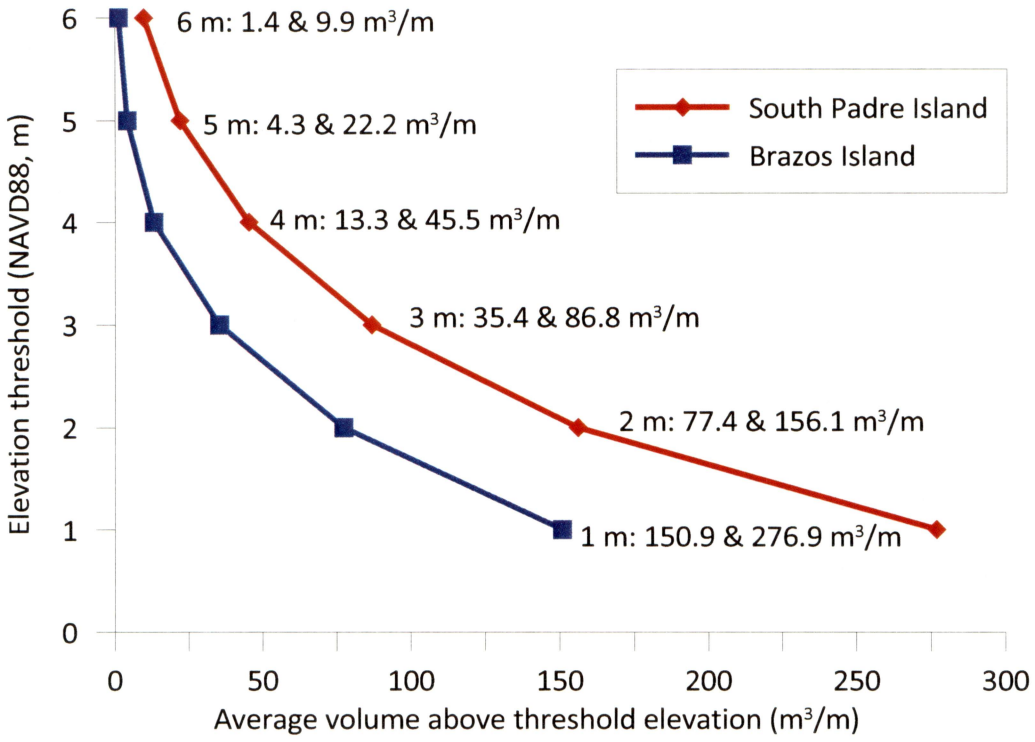

(b)

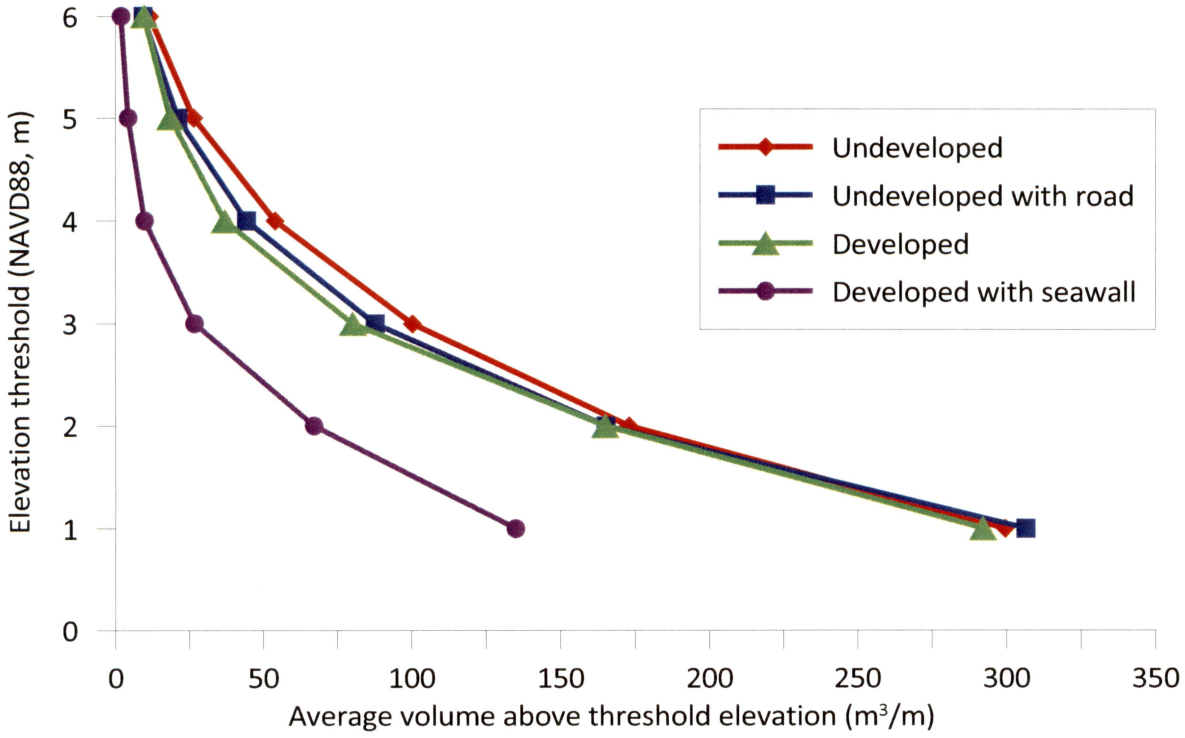

APPENDIX C: THRESHOLD ELEVATION CURVES-SHORELINE SEGMENT CHANGE

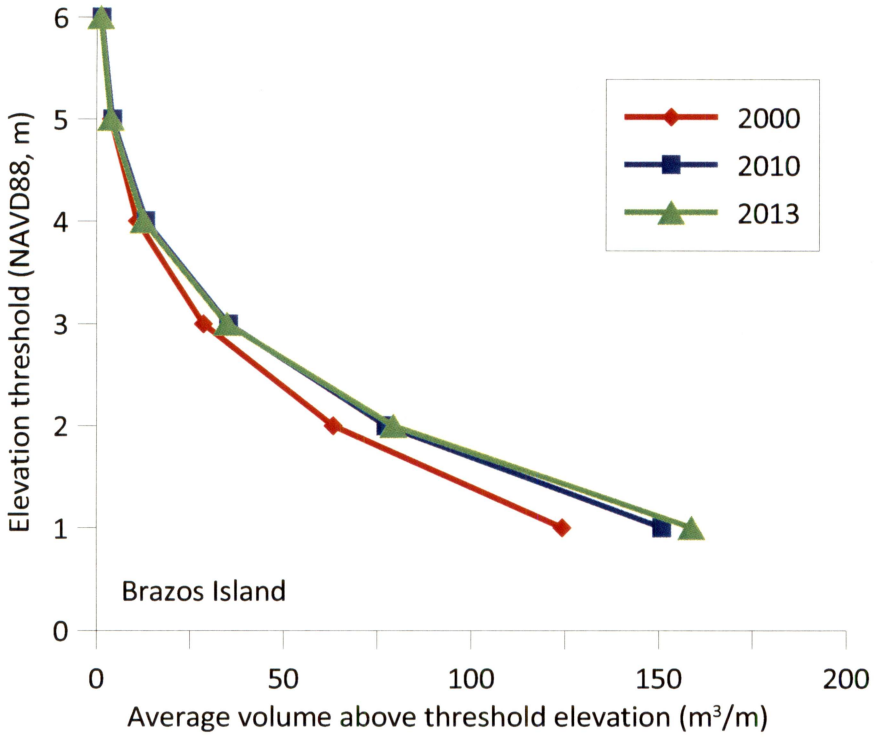

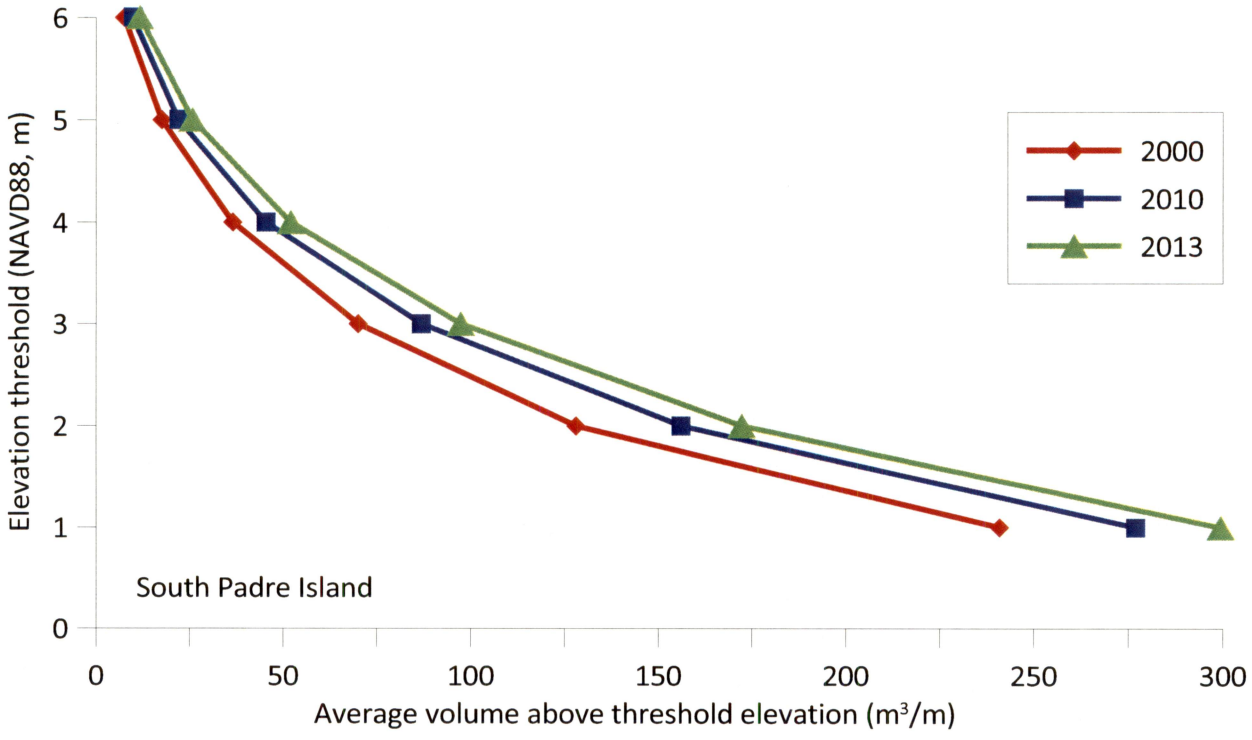

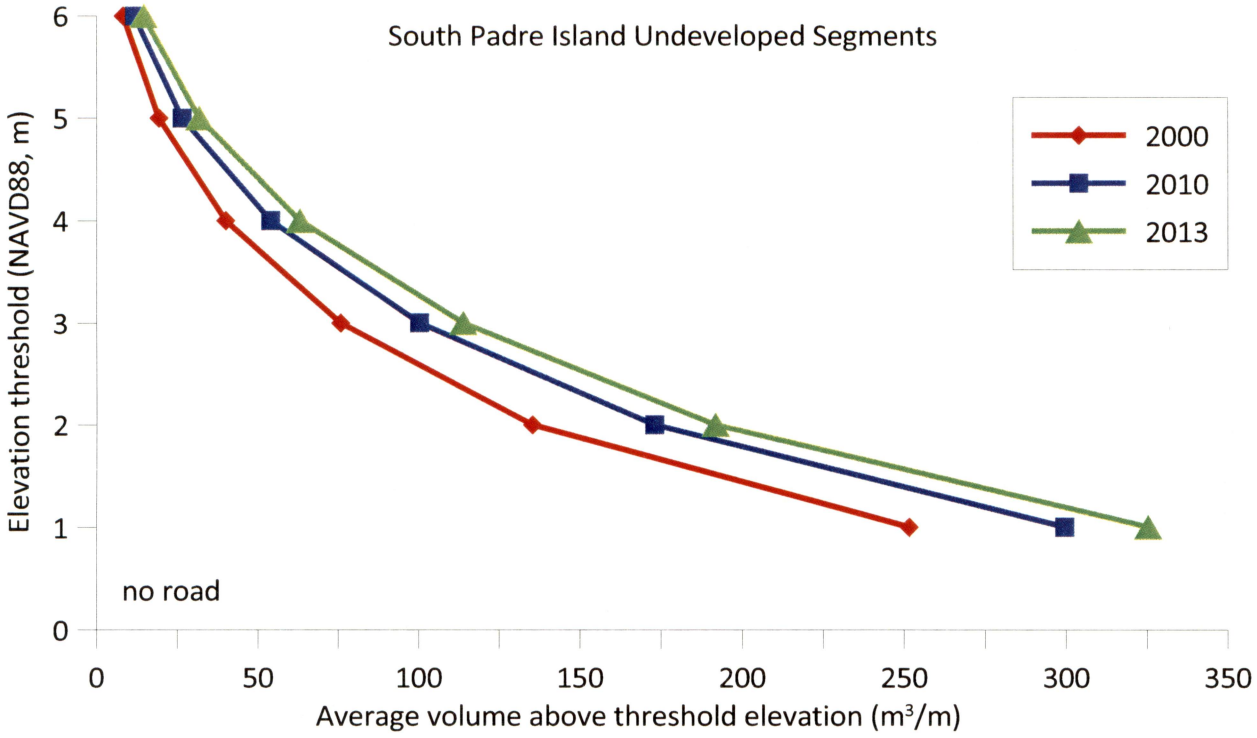
South Padre Island Undeveloped Segments
2000
2010
2013
Elevation threshold (NAVD88, m)
0
1
2
3
4
5
6
no road
0
50
100
150
200
250
300
350
Average volume above threshold elevation (m³/m)

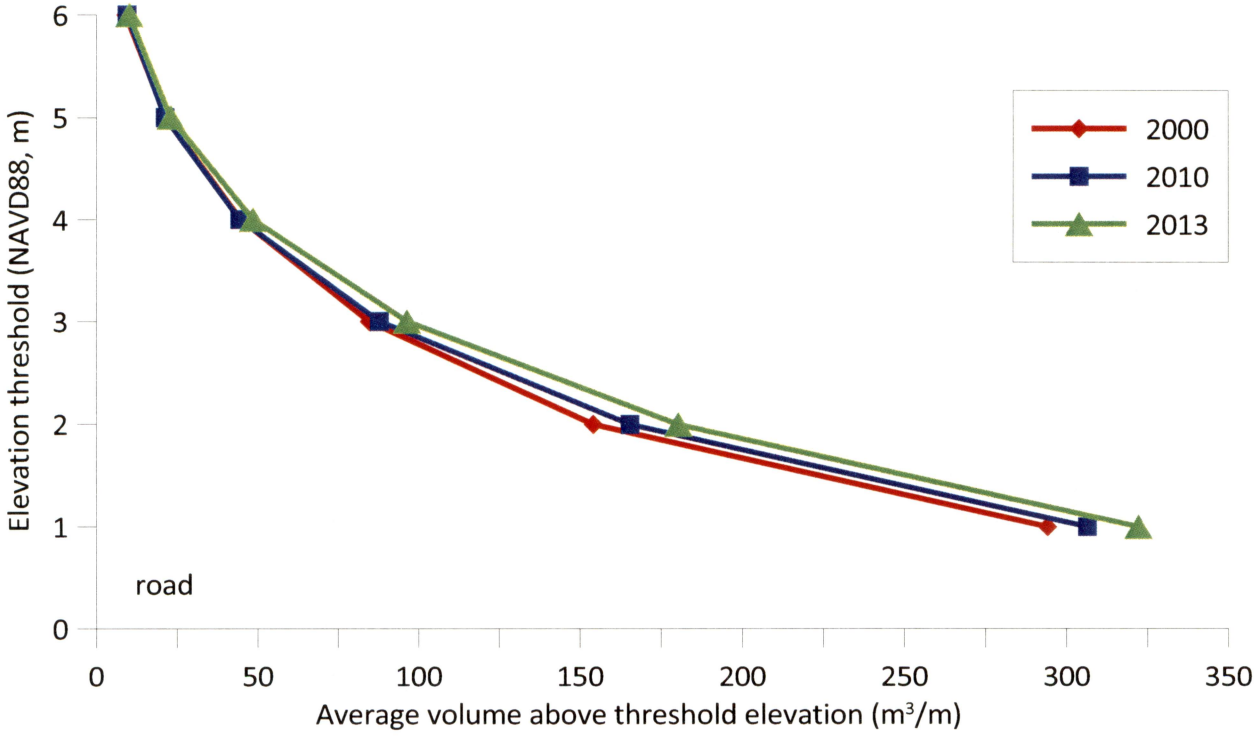
2000
2010
2013
Elevation threshold (NAVD88, m)
0
1
2
3
4
5
6
road
0
50
100
150
200
250
300
350
Average volume above threshold elevation (m³/m)

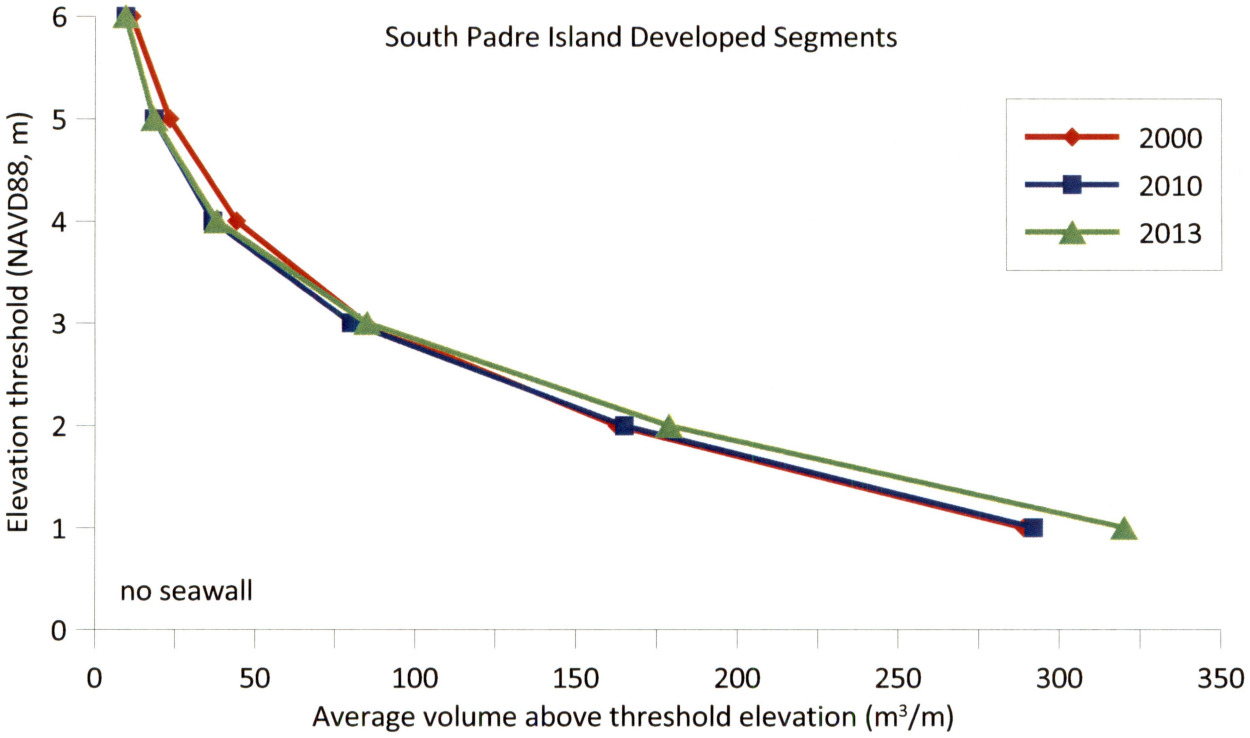
South Padre Island Developed Segments
2000
2010
2013
Elevation threshold (NAVD88, m)
0
1
2
3
4
5
6
no seawall
0
50
100
150
200
250
300
350
Average volume above threshold elevation (m³/m)

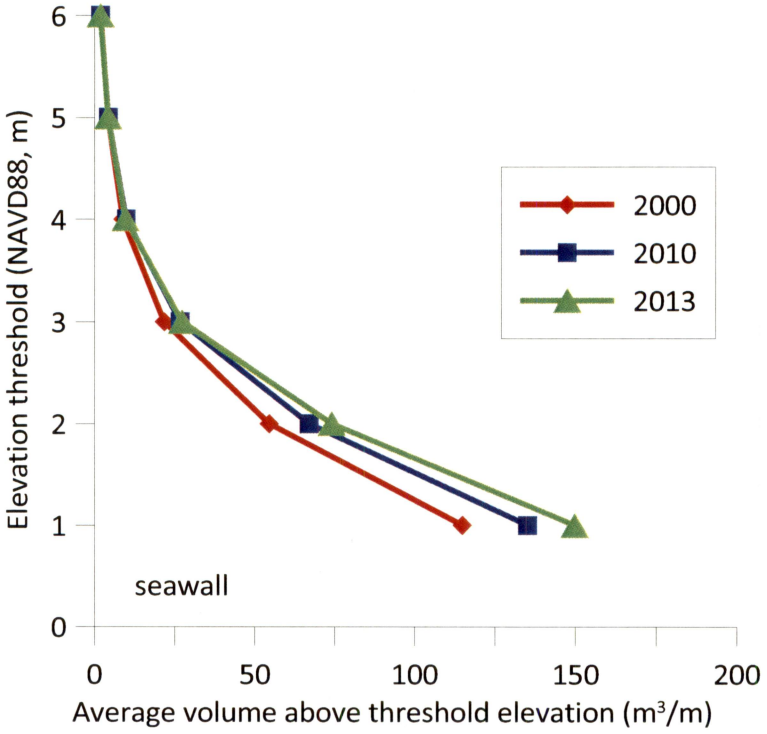
2000
2010
2013
Elevation threshold (NAVD88, m)
0
1
2
3
4
5
6
seawall
0
50
100
150
200
Average volume above threshold elevation (m³/m)

APPENDIX D: DATA VOLUME CONTENTS

The hard drive that accompanies the report contains the data acquisition report, GIS data deliverable report, a presentation, topographic and bathymetric lidar files, CIR aerial imagery and GIS files from the February 2013 airborne survey of South Padre Island and Brazos Island conducted by the Bureau of Economic Geology on behalf of the Texas General Land Office. The lidar and GIS products are final deliverables for the project titled "Acquiring Nearshore Bathymetric and Topographic Elevation Data and Aerial Imagery of South Padre Island, Texas," GLO contract number 13-030-000-6895.

All spatial data are in the UTM projection, World Geodetic System 1984 (WGS84), zone 14. Elevation and coordinate units are in meters. Elevation data are relative to the North American Vertical Datum 1988 (NAVD88).

A folder-by-folder description of the contents of the disk follow.

CMP-SPI-BATHYMETRY: contains February 2013 water surface and bottom returns LAS files, ASCII DEMs, and associated metadata for Port Isabel NE and South of Potrero Lopeno South East NE quarter-quadrangles.

CMP-SPI-GIS-FILES: contains ArcGIS shapefiles and Google Earth KMZ files representing maximum dune crest, landward dune line, geomorphic units, potential vegetation line, shoreline, beach and dune volume statistics, and long-term shoreline change rates.

CMP-SPI-PHOTOGRAPHY: contains February 2013 CIR aerial photography and associated metadata.

CMP-SPI-PRESENTATION: contains a pdf of a project related presentation given by T. L. Caudle at the 2013 American Shore and Beach Preservation Association National Coastal Conference in South Padre Island, Texas on October 24, 2013. Also contains presentation abstract.

CMP-SPI-REPORTS: contains Bureau of Economic Geology reports; (1) summarizing airborne data acquisition activities for February 2013, (2) summarizing GIS data deliverables derived from the aerial survey, and (3) high- and low-resolution versions of the final project report (this document) suitable for printing or on-screen viewing.

CMP-SPI-TOPOGRAPHY: contains February 2013 all-point topographic LAS files, an ASCII DEM, and associated metadata. Due to the size of the all-point data, LAS files are presented as quarter-quadrangle files.